PAUL SPRING: AN INVESTIGATION OF RECHARGE IN THE ROSWELL (N.M.) ARTESIAN BASIN *

by

Gerardo Wolfgang Gross
Professor of Geophysics
New Mexico Institute of Mining and Technology

Paul Davis
Graduate Research Assistant
New Mexico Institute of Mining and Technology

Kenneth R. Rehfeldt
Graduate Research Assistant
New Mexico Institute of Mining and Technology

PARTIAL TECHNICAL COMPLETION REPORT

Project No. A-055-NMEX

December 1979

New Mexico Water Resources Research Institute
in cooperation with the
Geophysical Research Center
New Mexico Institute of Mining and Technology

The work upon which this publication is based was supported in part by funds provided through the New Mexico Water Resources Research Institute by the U. S. Department of the Interior, Office of Water Resources Research and Technology, as authorized under the Water Resources Research Act of 1978, Public Law 95-467, under project number A-055-NMEX and by the State of New Mexico through State appropriations.

---

*Based in part on research performed by Paul Davis in partial fulfillment of the requirements for the degree of M. S. in Geoscience with specialization in Hydrology.

The purpose of WRRI technical reports is to provide a timely outlet for research results obtained on projects supported in whole or in part by the Institute. Through these reports we are promoting the free exchange of information and ideas and hope to stimulate thoughtful discussion and action which may lead to resolution of water problems. The WRRI, through peer review of draft reports, attempts to substantiate the accuracy of information contained in its reports but the views expressed are those of the author(s) and do not necessarily reflect those of the WRRI or its reviewers.

ABSTRACT

Paul Spring is the principal or sole discharge point of a perched localized aquifer of well defined boundaries. It is located on the western flank of the Roswell artesian basin, and conditions at Paul Spring are considered typical for a major portion of the basin. The recharge at Paul Spring could therefore provide insight into the recharge mechanisms controlling the basin's groundwater supply. The geology of the area was mapped in detail. Springflow was measured over a span of 453 days. Precipitation records of many years were available from a NOAA weather station in the area. Tritium was measured in spring discharge and precipitation. Numerical and stochastic analysis and cross-correlation were performed on the data. The results suggest that a deep flow component plays an important role, hitherto underestimated, in the groundwater recharge to the basin. This deep component is transmitted by the Permian Yeso Formation and the Glorieta Sandstone Member of the San Andres Formation. At Paul Spring, this accounts for as much as 80% of the discharge. No clear results were obtained for the Paul Spring aquifer's response time to precipitation events. The indications are that it is of the order of several months. This can be explained by the peculiar geologic structure, specifically the screening effect of the Glorieta sandstone, in combination with solution and collapse features in the Yeso formation which channel the recharge water. A longer series of springflow measurements under better controlled conditions is needed to clarify this problem. The measurements continue.

TABLE OF CONTENTS

Page

LIST OF FIGURES

LIST OF TABLES

ACKNOWLEDGMENTS

The authors are pleased to acknowledge the assistance of numerous individuals instrumental in the completion of this study.

Paul Spring and the area around it is owned by Mr. Charles Mulcock. Mr. Mulcock and his family not only gave permission for the study to be done on their land, but also helped install and maintain the springflow recording system, provided precipitation records for the area, and contributed generously of their vast knowledge of the area. Without their help this study could not have been accomplished.

Ralph Wilcox, Chris Duffy and Rich Naff assisted in all phases of this study, from construction of the recording system to advising on technical aspects of the project.

Scott Anderholm and James Counts helped with geological mapping and sample collection. Gerald Mitchell provided information pertaining to the soils of the Paul Spring area. Aerial photographs were taken by David Dorschner. Charlie Mumma and Prof. Allan Gutjahr assisted in the spectral analysis section of this report. Prof. Lynn Gelhar suggested methods of analysis and reviewed the manuscript. The responsibility for errors or omissions rests with the authors.

PURPOSE AND JUSTIFICATION

The purpose of this investigation was to determine the amount and percentage of precipitation which recharges the Paul Spring aquifer. Paul Spring is situated near the southwestern edge of what has been referred to as the Principal Intake Area (Fiedler and Nye, 1933). This area recharges the Principal Aquifer of the Roswell artesian basin, the San Andres Formation. Factors which affect recharge at Paul Spring appear to be typical for the Principal Intake Area.

A combination of four felicitous factors determined the choice of Paul Spring for this study: (1) The spring's owner, Mr. Charles Mulcock, graciously gave his permission for the installation of necessary equipment. (2) The spring configuration is such that a weir and stilling well could be installed relatively easily. (3) The location of the spring is protected from access to vandals and cattle. (4) A preliminary study indicated that Paul Spring was the principal, if not the only outlet of a small perched aquifer of rather well defined boundaries.

The outflow from the system is assumed to be equal to the springflow. This assumption neglects transpiration from phreatophytes and possibly downward leakage of ground water through the semi-confining bottom layer of the perched system. The only phreatophytes which tap the Paul Spring aquifer are located near the point of issuance of the spring. They consist of several cottonwood trees, the amount of water they transpire is believed

to be small; it is therefore neglected.

The stratigraphic layer which forms the bottom of the Paul Spring aquifer is composed of fine silts and some clay. It is not possible to determine the amount of water which flows vertically downward through this layer. Neglecting this flow (which otherwise would contribute to the spring) should yield a minimum value for the amount of recharge to the system.

LOCATION, PHYSIOGRAPHY, AND CLIMATE

Paul Spring is located in Chaves County, southeastern New Mexico (Figs. 1, 2). The exact location is given by the coordinates T16S.R16E.11.34213, using the New Mexico State Engineer method of locating wells and springs (Fig. 3). This perennial spring issues from a perched water body contained in a hill on the southeastern flank of the Sacramento Mountains. The hill makes up most of the area covered in this report.

Fig. 2 is a sketch map of the area we call the Roswell basin in this report. It is a sub-basin of the much larger Pecos drainage basin. It is physiographically limited by the Pecos River and the Sacramento Mountains on the east and west flanks, respectively. The mostly dry Arroyo del Macho is the northern boundary, and the Seven Rivers Hills near Carlsbad are the southern limit. The northern and southern boundaries are somewhat arbitrary in that they may not be hydrologic boundaries. Their choice is, however, justified by the surface extension of Fiedler and Nye's Principal Intake Area. It is shown in relation to the total area (enclosed by the dotted line) which, according to Bean (1949), contributes to the artesian groundwater basin. This region extends about 30 miles further north than the area shown in Fig. 2.

The amount of precipitation and the fraction of precipitation that becomes recharge are directly related to the physiography of a given area. The climate controls the amount of water available

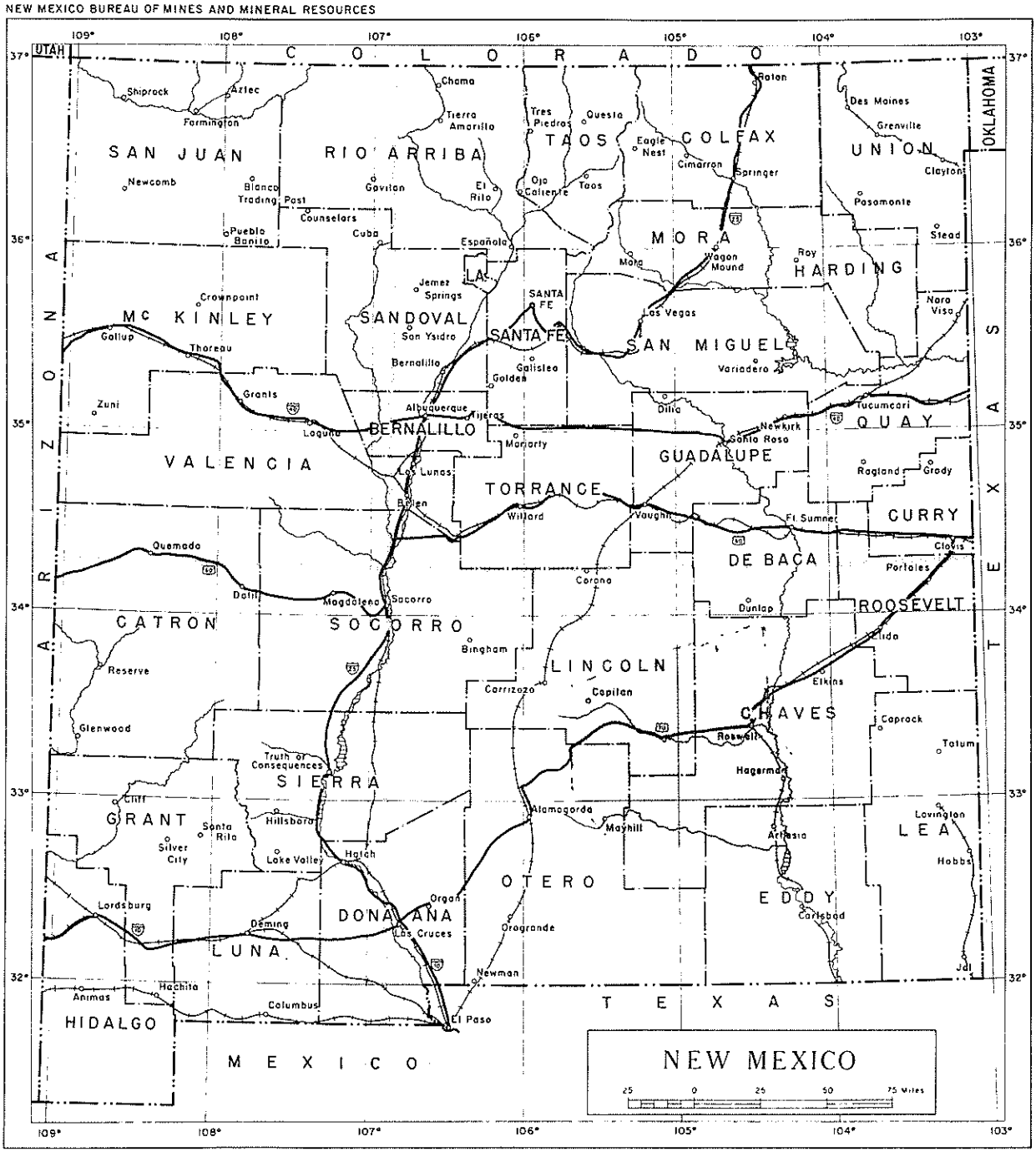

Fig. 1. Location of the study area

for recharge, and the physiography has some control over the percentage of water that actually reaches the ground water system.

Climatically the study area lies between the semi-arid plains to the east, near Artesia, and the sub-humid region of the east flank of the Sacramento Mountains to the west. The average annual rainfall is 16 inches (Table I), most of which falls during thundershowers in the summer months. Winters are usually mild with light snowfall. The area is characterized by plentiful sunshine, large daily temperature fluctuations, and low relative humidity. Precipitation for the period from August 1972 to March 1978 is shown in Fig. 4. These values are from the Elk, New Mexico, weather station which is within less than a mile from Paul Spring.

The southeastern flank of the Sacramento Mountains is part of the eastward tilted fault block known as the Sacramento uplift (Kelley, 1971). The ridge containing the perched water body trends southwest to northeast (Fig. 6). This area is drained by two arroyos, one in Paul Canyon and one in Short Canyon, which both empty into the Rio Peñasco. The Rio Peñasco is a major drainage of the southern Sacramento Mountains and flows perennially in the area of Paul Spring.

Local relief within the study area is as much as 500 feet between Paul Canyon and the crest of the ridge. The elevations above mean sea level range from 5670 feet at the nearly horizontal alluvial flood plain of the Rio Peñasco to almost 6500 feet in the southwestern portion of the study area.

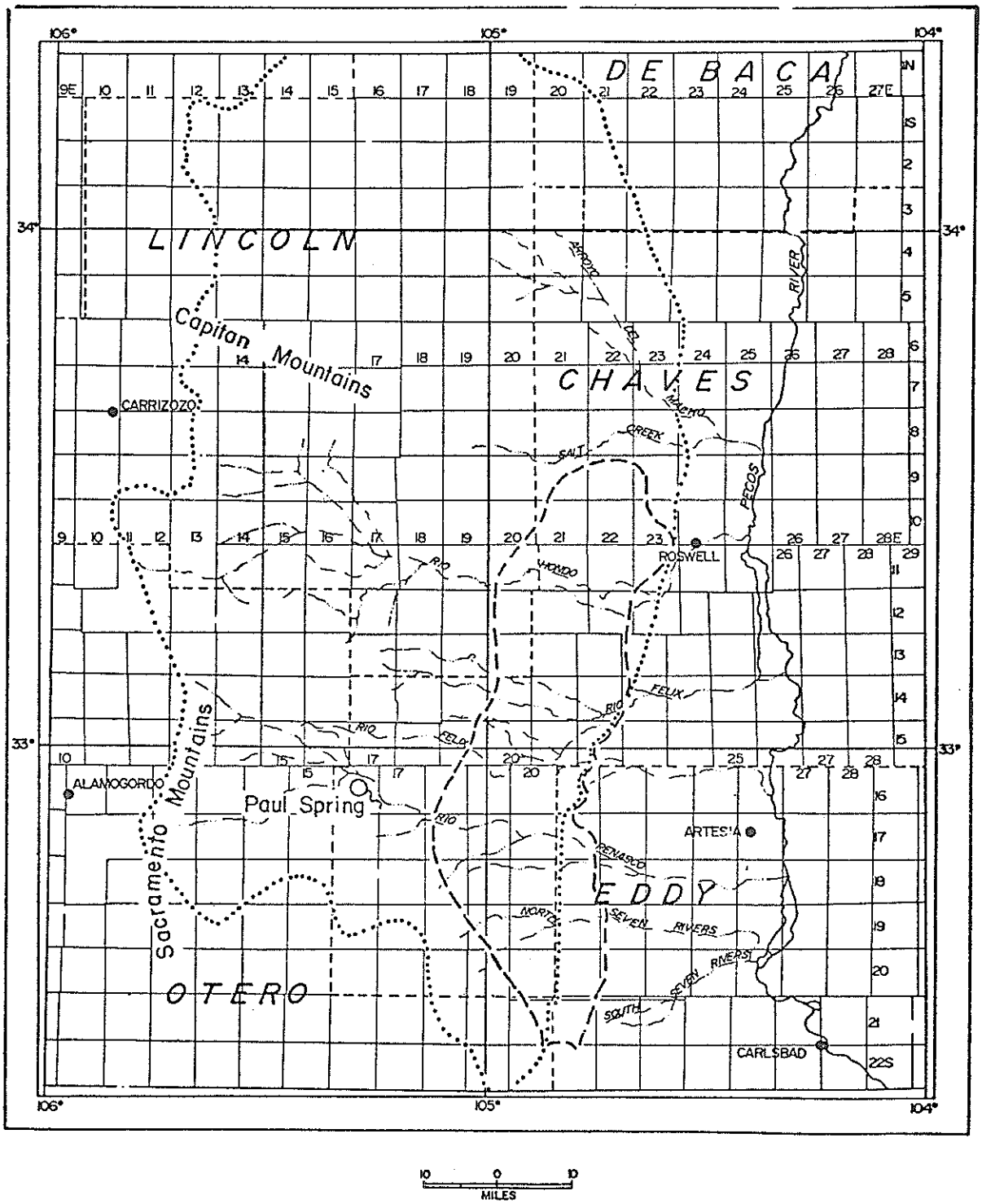

Fig. 2. Location of Paul Spring in relation to the Roswell artesian basin. Dotted line: total intake area (Bean, 1949). Dashed line: Principal Intake Area (Fiedler and Nye, 1933).

Table I. Annual Precipitation for Elk, Roswell, and the Roswell Artesian Basin.

Year	Precipitation in Inches			Average Temp. °F	
	Elk	Roswell	Roswell-Artesian Basin Average	Elk	Roswell
1955	17.78	8.75	13.77	57.8	59.9
1956	8.75	4.32	7.56	54.4	60.3
1957	18.37	9.32	13.88		60.5
1958	22.86	13.06	19.35	53.5	60.3
1959	10.43	9.52	12.16	54.0	60.1
1960	17.23	13.57	14.13	53.1	58.8
1961	13.89	7.85	12.40	53.3	57.9
1962	20.62	11.81	14.79	53.9	58.8
1963	15.77	6.30	9.08		59.3
1964	8.84	6.98	8.88		58.9
1965	14.03	6.68	13.82	53.6	60.0
1966	18.19	9.68	12.92	53.0	58.8
1967	11.45	11.06	11.43		59.1
1968	20.80	15.84	15.47	53.5	57.6
1969	18.89	13.33	15.64	54.8	60.3
1970	9.45	8.63	9.65	54.3	58.9
1971	13.57	10.04	14.16		59.6
1972	20.97	16.24	20.33	55.0	
1973	10.37	11.60	11.10	53.0	59.3
1974	26.51	18.65	20.07	53.0	60.0
Average	15.88	10.66	13.53	54.09	59.39

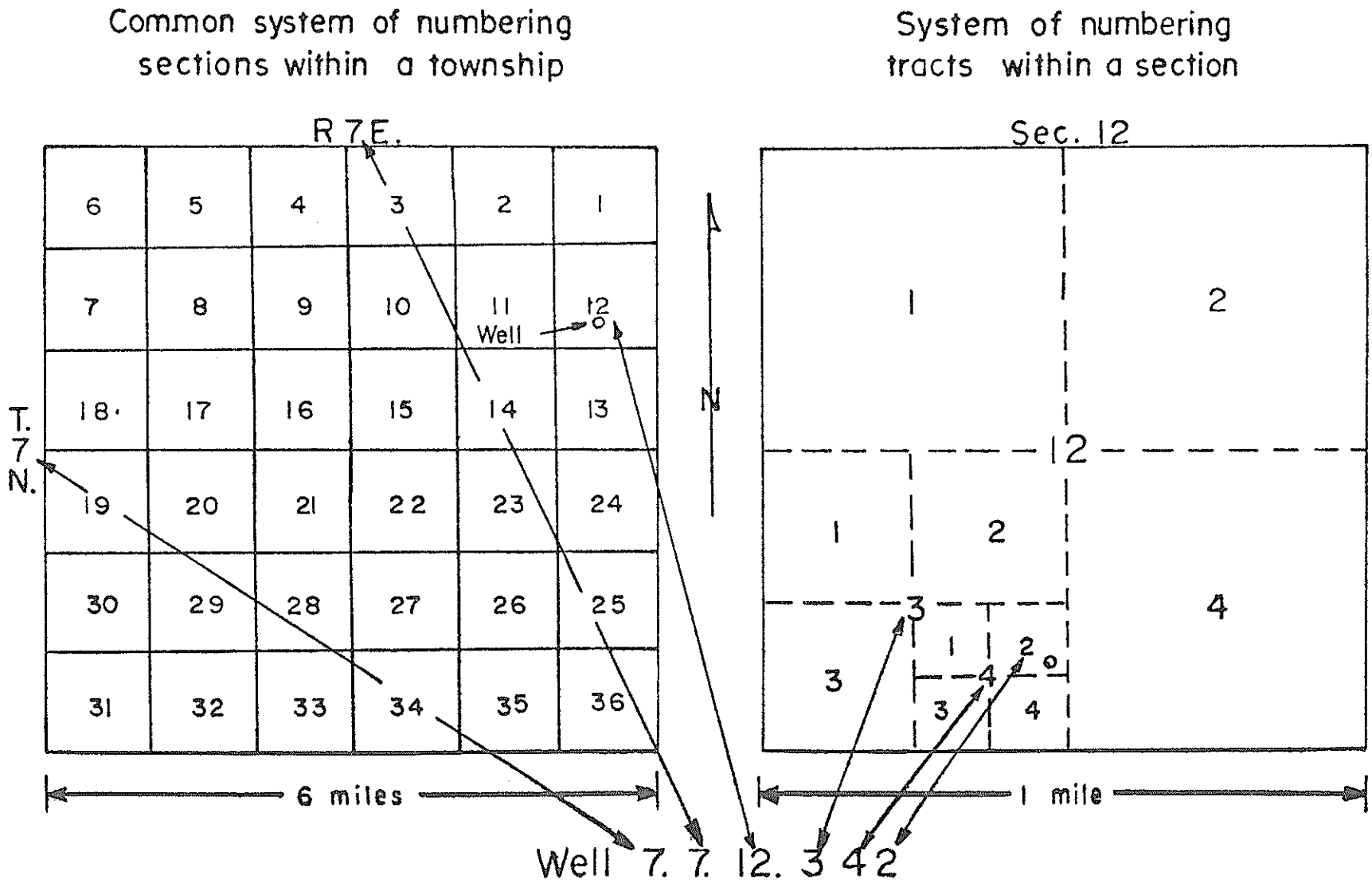

Fig. 3. Coordinate system for locating wells and springs.

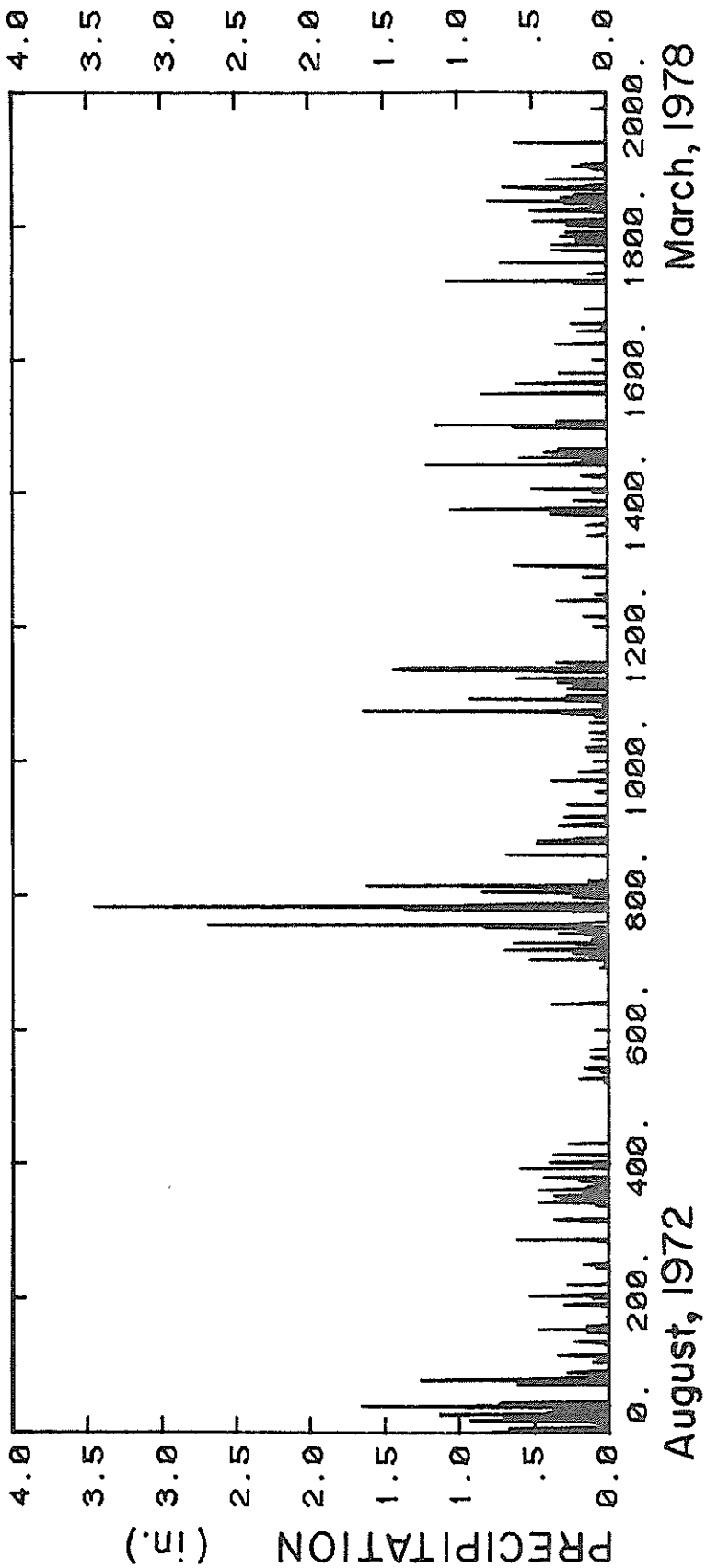

Fig. 4. Precipitation at the Elk weather station.

HYDROGEOLOGIC SUMMARY

The hydrologic problems of the Roswell basin were discussed in some detail by Gross et al. (1976). An updated report is in preparation (Gross and Hoy, 1979). The purpose of the following hydrogeologic summary is to indicate the place of the Paul Spring study in the hydrogeologic investigation of the basin as a whole.

A simplified stratigraphic column is given in Table III. The Principal Aquifer of the Roswell basin is the San Andres Limestone which forms the dipslope on the east side of the Sacramento Mountains along their base. Along the west bank of the Pecos River, between Roswell and Artesia, the San Andres and Artesia are unconformably covered by a complex, up to 500 ft thick, of late Tertiary to early Pleistocene sandstones (Gatuna Formation) and Pleistocene to Holocene alluvium. These strata form a strip about 20 miles wide and contain the Shallow, or water table, Aquifer.

The Artesia Group covers the San Andres along the east bank of the Pecos River.

The Principal Aquifer receives recharge in three longitudinal zones, at successively lower elevation, between the Sacramento Mountains in the west and the Pecos River to the east.

(1) Winter and summer precipitation falling in the mountains west of R 19 E (Fig. 2) is absorbed by the San Andres and underlying formations, notably the basal Glorieta Sandstone of the San Andres and the Yeso Formation. Moving eastward, this water rises with the water table into the upper San Andres and becomes the unconfined

western part of the Principal Aquifer where the San Andres forms the dipslope; the latter is most fully developed in Fiedler and Nye's Principal Intake Area.

(2) Part of the precipitation falling in the western mountains runs off through the four major tributaries of the Pecos River in the study region, from north to south, Arroyo del Macho, Rio Hondo, Rio Felix, and Rio Peñasco. (Paul Spring belongs to the last-named.) As they cross the Principal Recharge Area, these streams lose all or most of their flow due to the karstic character of this zone. This is the second recharge component, and it has been studied in some detail in the Rio Hondo, the largest tributary to the Pecos in this area (Duffy et al., 1978).

(3) The Principal Recharge Area receives little winter precipitation. Summer thunderstorms supply the bulk of its surface moisture. It presumably contributes to recharge, especially in the relatively flat, karstic interfluvial highlands.

(4) The alluvial plain on the west bank of the Pecos River has major agricultural developments. Large-scale irrigation takes most of the water from the Principal Aquifer, which is confined in this zone; the resultant depression of the piezometric head causes leakage from the alluvial aquifer into the San Andres Limestone. This leakage consists of groundwater from the alluvial aquifer as well as of irrigation return flow.

(5) The depression of the piezometric head in the Principal Aquifer is cause of a saltwater invasion which advances on a NW-SE

front from the northeast and has reached the city limits of Roswell. The progressive decline of piezometric head and of water quality are the major problems facing the basin communities. An assessment of the different recharge contributions is a necessary step if a model of the basin is to be constructed. Ultimately, such a model should help in alleviating the problems just mentioned. Recharge supplied at different elevations is characterized, in principle, by different isotopic composition which can be used to identify and to trace the several contributions. This is one purpose of the present and related investigations.

PREVIOUS RECHARGE INVESTIGATIONS

The earliest and only study which deals with the immediate area around Paul Spring was done by Renick (1926). He described the general geology and ground water conditions of the Rio Peñasco above Hope. Paul Spring was described as being one of the Boyd Williams Springs. Renick also gave a geologic cross section of the spring (Fig. 5) and a chemical analysis of the spring water (Table II). The cross section given by Renick (Fig. 5) in no way resembles the cross sections constructed from geologic mapping done during this study (Figs. 7-9).

A complete geologic and hydrogeologic study of the Roswell artesian basin was published by Fiedler and Nye in 1933. They included estimates of the quantity of recharge and of the recharge fraction (the percentage of precipitation which becomes recharge water) for the entire Roswell basin. They delineated an area which they believed contributed the most water to the recharge of the Roswell artesian aquifer. This area they referred to as the Principal Intake Area (Fig. 2). They defined this area to be bounded on the east by the line of contact between the Artesia Group and the San Andres Formation.* The western boundary was approximately drawn where the water table crosses the Yeso-San Andres Formation contact. Fiedler and Nye (1933) assumed that, since the Yeso Formation is relatively impermeable, ground water which was derived from precipitation west of this line would not percolate eastward and contribute to the artesian basin. The major contribution

*Probably, the contact between Gatuna and San Andres. The latter has frequently been included with the Artesia Group (Kelley, 1971, p. 31).

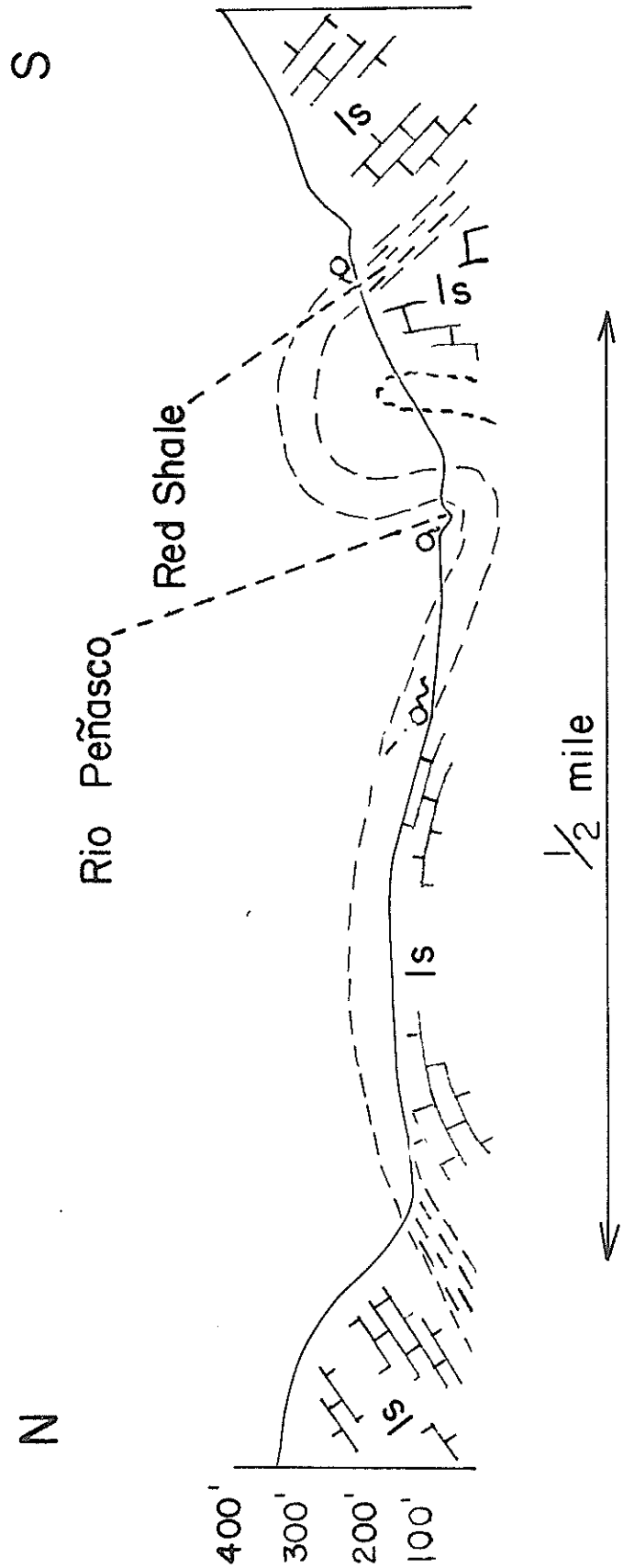

Fig. 5. Geologic cross section of Sec. 11, T.16S, R.16E. After Renick (1926). Three springs are shown. They were called Boyd-Williams Springs at the time of Renick's report. The southernmost spring is the present Paul Spring.

of water from the western region was believed by Fiedler and Nye (1933) to be from eastward flowing streams which lost their flow in the Principal Intake Area.

The recharge contribution from streams of the western portion of the Roswell basin has been studied by Bean (1949) and Mourant (1963). Hantush (1955) calculated the total quantity of recharge for the Roswell artesian basin. Some of his results are discussed below. Duffy et al. (1978) investigated recharge from the western region in the form of stream losses and percolation from the Glorieta Sandstone and Yeso Formation.

Ground water studies involving the use of tritium data have been presented by Rabinowitz et al. (1977), and by Gross et al. (1976).

The first of these studies was based entirely on tritium measurements of precipitation and of wells located in the confined part of the Principal Aquifer and in the covering alluvium. One of the recommendations of this work was that groundwater from the Principal Recharge Area should be investigated systematically; preliminary results were reported in the second study cited above. They indicated that a substantial fraction of the groundwater in the unconfined part of the Principal Aquifer was not derived from local precipitation and infiltration. Therefore it must come from deeper aquifers which receive their recharge in outcrop areas further west.

Table II. Chemical Analyses of the Paul Spring water, ppm. Comparison of data from 1926 and 1978.

Constituent	Date Collected	
	1926*	April 2, 1978
$CO_3^{=}$	0	0
HCO_3^{-}	226	223
Cl^{-}	8	1.0
$SO_4^{=}$	27	100
NO_3^{-}	.40	
Fe	.26	
SiO_2	15	
Na^{+}	9.4	6.0
K^{+}	9.4	.35
Mg^{++}	16	13.8
Ca^{++}	55	88
TDS	366.5	432.2

*From Renick (1926)

The hydrogeologic studies by Havenor (1968) and Kinney et al. (1968), though not directly concerned with recharge, are fundamental to an understanding of the basin hydrology and of its problems. Similarly important is the detailed description of the surface geology and geologic map by Kelley (1971).

The lumped parameter approach to phreatic aquifer modeling has been treated by several authors including Dooge (1960), Eriksson (1970) and Gelhar and Wilson (1974). Stochastic treatment of the lumped parameter model was first developed by Gelhar (1974) and then presented again by Flores and Gelhar (1976).

RECHARGE ESTIMATES

Following Fiedler and Nye (1933), recharge for the Roswell artesian basin has been assumed to come mainly from the Principal Intake Area, with the western portion of the basin contributing mainly runoff, which is lost through channel leakage in the Principal Intake Area. They considered that other contributions from the western area were not important because ground water is in the Yeso Formation, which is relatively impervious. They also felt that water moving along the Yeso-San Andres contact would contribute to surface water flow on the western flank of the basin and thereby to recharge in the Principal Intake Area. This would be the case for Paul Spring if its waters were not used for domestic purposes.

Fiedler and Nye (1933, p. 246) used an estimate of the total natural outflow of the basin, prior to ground water development, as the recharge amount. This amount they calculated at 250,000 acre-ft/yr. The percentage of precipitation which becomes recharge was then calculated to be 7.3 for the "total recharge area" (estimated by Fiedler and Nye as 4,000 square miles) or 29% for the Principal Intake Area (1,200 square miles). They suggested that the true value was probably less than 25% of precipitation falling on the Principal Intake Area and that the remainder was derived from streams which lose most of their flow in the Principal Intake Area.

Another approach to the calculation of the recharge for the Roswell artesian basin was taken by Hantush (1957). Hantush considered years when he felt the system was in "dynamic equilibrium",

that is inflow was equal to outflow. He also incorporated the concept of effective precipitation proposed by Jacob (1944). The effective precipitation is equal to "the rate of precipitation which, had it been maintained uninterrupted throughout the past, would have produced the same water table profile as actually existed at that particular time." Following Jacob, Hantush used the equations

$$\text{Recharge} = 21{,}000 \text{ (ac-ft/in)} \; \bar{R}_n$$

where the effective precipitation

$$\bar{R}_n = \sum_{i=1}^{K} \frac{2(K + 1 - i)}{K(K + 1)} R_{(n + 1 - i)}$$

and

R = measured precipitation (Hantush used Roswell and Artesia data)

K = 3 = number of years that rainfall of a given year is effective (Hantush, 1957, p. 49).

Hantush arrived at a figure of 240,000 acre-ft/yr for the years considered by him (viz.: 1928, 1936, and 1944).

We can estimate a recharge percentage using Hantush's approach as follows. The average annual precipitation in the Roswell Basin for the years 1975, 1976, 1977, calculated with the Thiessen polygon method as given by Gross et al. (1976), was found to be 11.71, 12.51, and 12.01 inches, respectively. From Hantush's equation, the effective precipitation, $\bar{R}_n$, was calculated as 12.13 inches/year = 1.011 ft/yr. The total basin area, $\underline{A}$, is 8,243 mi^2 = 2.3×10^{11} ft^2 (from Gross et al., 1976, p. 182). Hence, the mean

yearly volume of precipitation falling on the basin is 5,300,000 acre-ft. Also, from Hantush's formula, the effective precipitation or total recharge volume is

$$\bar{\bar{R}}\bar{n} = 21{,}000 \times 12.13 = 250{,}000 \text{ acre-ft}$$

and the recharge fraction

$$r = \frac{250{,}000}{5{,}300{,}000} = 0.047 \text{ or } 4.7\%.$$

In estimating this percentage we have used the total basin area computed by Gross et al. (1976). Hantush's computation of total recharge volume did not involve the basin area (Hantush, 1957, p. 52). In fact, Hantush does not define the basin area in his report. If we assume Fiedler and Nye's total recharge area (4,000 square miles) the recharge percentage, calculated with Hantush's formula, would become about 9.7%. Whereas the estimates of effective precipitation by Fiedler and Nye, by Hantush, and by the above approach which is based on Hantush's formula all give a value close to 250,000 acre-ft, the estimates of recharge fraction, which involve the surface area over which effective precipitation takes place, vary over a wide range.

Duffy et al. (1978, p. 58) estimated the total contribution of the western region to be approximately 133,000 acre-feet/yr. This calculation represents underflow contributed by the Yeso Formation and the Glorieta Sandstone, which was assumed negligible by Fiedler and Nye (1933). The validity of including this flow will be discussed in a following section dealing with tritium measurements.

This underflow contribution is included in both Fiedler and Nye's and Hantush's recharge calculations because they consider total basin outflow at equilibrium as a measure of recharge. Thus, the contribution to recharge from precipitation on the San Andres Formation (and the overlying alluvium) should be less than one half of total recharge. This further reduces the recharge fraction as estimated above.

These considerations serve to underscore the importance of underflow from formations underlying the San Andres (viz.: Yeso), as opposed to precipitation and direct infiltration, for the basin's hydrologic budget.

PROCEDURE

In order to estimate the amount of precipitation that contributes recharge to the Paul Spring groundwater system, the following basin characteristics and parameters had to be defined or measured: hydrologic boundaries of the local basin, hydrogeologic characteristics, local recharge area, hydrologic connections of the local aquifer with adjacent systems; precipitation input, outflow, correlation of tritium measurements of precipitation and groundwater.

Hydrogeology

In order to determine hydrologic boundaries, hydrogeologic characteristics, recharge area, and hydrologic connections, the area was mapped in detail on a U.S.G.S. topographic map which was expanded to a scale of 1:800. The use of several air photographs in color supplemented the field mapping. The geologic map was reduced in scale and is reproduced in Fig. 6. The recharge area and hydrologic conditions were then delineated by considering the geologic constraints of the system.

Precipitation

Precipitation records from Elk (Fig. 4) were used for this study. The rain gauge is located within less than a mile of the local recharge area.

Outflow

The outflow from the system was assumed to be equal to the

discharge of Paul Spring. To measure it, a stilling pond was dug and equipped with a weir and a water level recorder. A continuous record of springflow was obtained during 453 days. The details of construction, measurement procedures, and problems encountered are given in Appendix B. The measurements are tabulated in Appendix C.

The precipitation and discharge data were used to compute recharge by a lumped parameter approach. These computations will be discussed in detail.

Tritium Determinations

These measurements were carried out at the Tritium Laboratory of New Mexico Institute of Mining and Technology as part of a systematic basinwide investigation. A comparison of tritium values in precipitation and groundwater was to yield clues concerning residence times and circulation patterns. A detailed discussion of measurement techniques, sampling procedures, and basinwide results is given in previous reports (Rabinowitz and Gross, 1972; Gross, et al., 1976).

GEOLOGY OF PAUL SPRING

Particular attention was paid to the geology in order to define the area of recharge for the Paul Spring aquifer. Two formations of Permian age are exposed along with several Quaternary units. Their surface distribution is shown on the geologic map (Fig. 6).

Figs. 7, 8, and 9 give cross sections through the study area. The stratigraphic column is given in Table III.

The Permian System

Yeso Formation

The Yeso Formation is the oldest rock unit which crops out in the study area. It is of particular hydrogeologic importance because it forms the semipermeable bottom as well as part of the aquifer of the perched system.

In the region covered by this report the Yeso is exposed along the base of the central and northeast portion of the ridge containing the perched water body.

Very friable reddish and yellowish siltstones in the upper part of this formation form the semipermeable layer holding up the perched water system. Exposures of thinly bedded limestone or dolomite which contain chert nodules are also common in this area. Significant amounts of gypsum occur in the upper Yeso Formation (Kelley, 1971). Although gypsum was not encountered in field mapping of this region, its subsurface presence is indicated by the high sulfate content in the water issuing from Paul Spring (Table I).

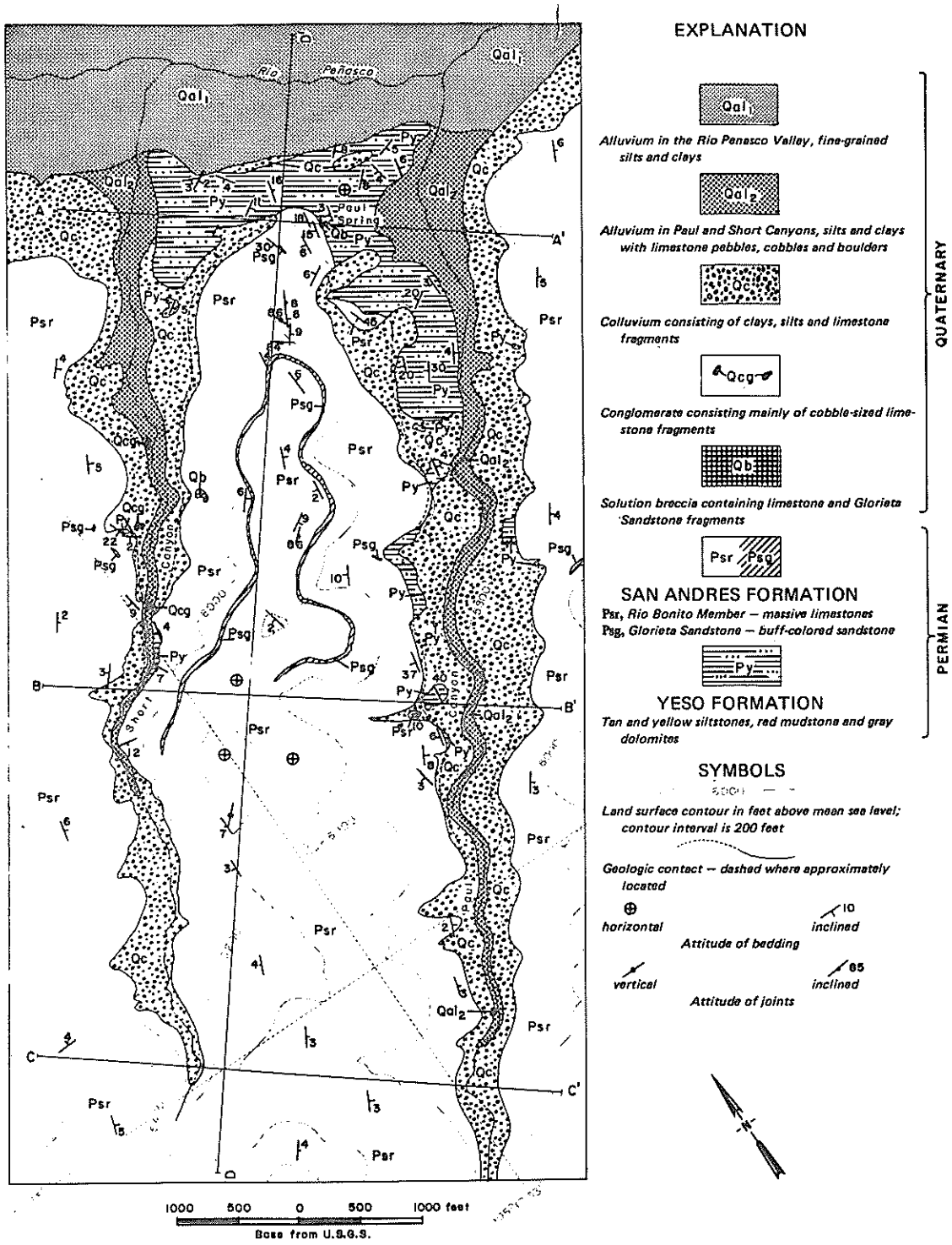

FIGURE 6 — GEOLOGIC MAP OF THE PAUL SPRING AREA, CHAVES COUNTY, NEW MEXICO

In this area, Yeso outcrops are commonly disturbed by collapse. Dissolution of gypsum in the upper part of the Yeso Formation could have caused these collapse features which are abundant near the Yeso/San Andres Formation contact.

Since only the upper portion of this formation is exposed, it was not possible to measure its thickness.

San Andres Formation

The San Andres Formation conformably overlies the Yeso Formation in this region. It makes up the major part of the hill containing the perched water body and is the formation through which precipitation must infiltrate to recharge the perched system. In the area covered by this report the San Andres is represented by the Glorieta Sandstone Member and a portion of the Rio Bonito Member.

The Glorieta Sandstone occurs as an intertonguing unit within the Rio Bonito Member. There are two lenses of this sandstone which crop out in the study area. Both are similar in composition being medium grained, well sorted, moderately cemented, tan quartz sandstones. The lower sandstone tongues in and out near the Yeso-San Andres contact. It averages about two feet thick and at one location grades into a thin, yellow, friable siltstone below it. The upper sandstone occurs as a lens about 180 feet above the Yeso-San Andres contact. This sandstone is approximately 20 feet thick in the northeast part of the area and gradually thins until it pinches out in the central part of the study area (Fig. 9).

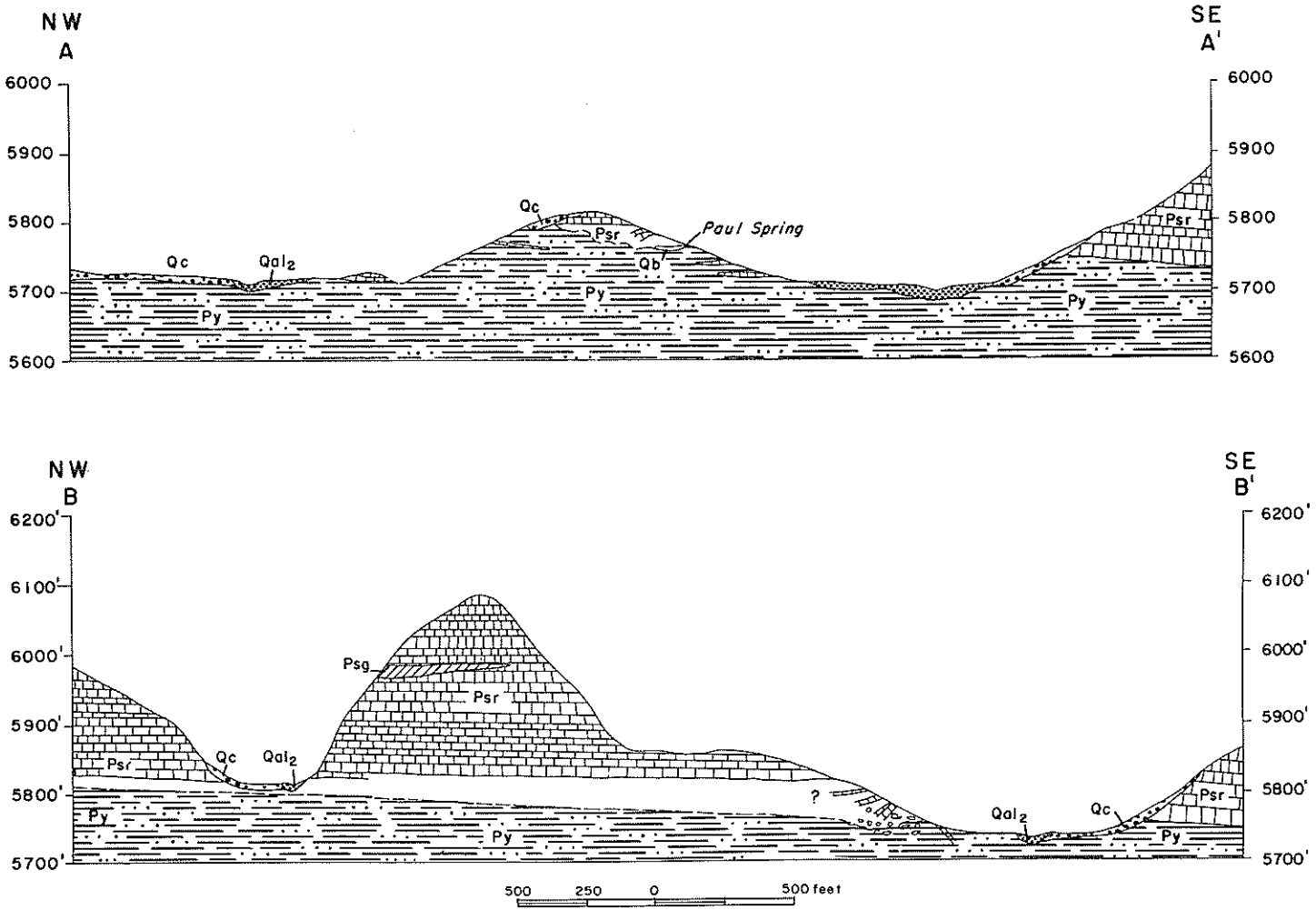

FIGURE 7 — GEOLOGIC CROSS SECTIONS A – A', B – B'

The Rio Bonito Member is exposed throughout most of this area. It consists of highly jointed limestone beds which are usually 3 to 6 feet thick and exhibit markedly parallel bedding. Some beds occur which are 10 and 20 feet thick. Since the upper boundary of this unit is not encountered in this study, an accurate total thickness cannot be reported.

The Quaternary System

Conglomerate Unit

This unnamed unit occurs as isolated outcrops only near the dry stream bed in Short Canyon. It consists of mainly sub-angular to sub-rounded fragments of locally derived limestone in a matrix of sand, silt and clay, moderately cemented by caliche. It was probably deposited in Paul Canyon also, but later eroded away as the area underwent renewed uplift.

Solution Breccia Unit

This unit is also unnamed and occurs as isolated outcrops. It is the unit from which Paul Spring issues. At Paul Spring it contains angular boulders, cobbles, and pebbles of limestone, and angular fragments of tufa in a calcite-cemented matrix of finer limestone particles. These limestone fragments were probably derived from the San Andres Formation. This unit also occurs in the north-central part of the area and consists of angular fragments of limestone and Glorieta Sandstone in a matrix similar to the breccia at Paul Spring. It is difficult to determine when this solution breccia began forming

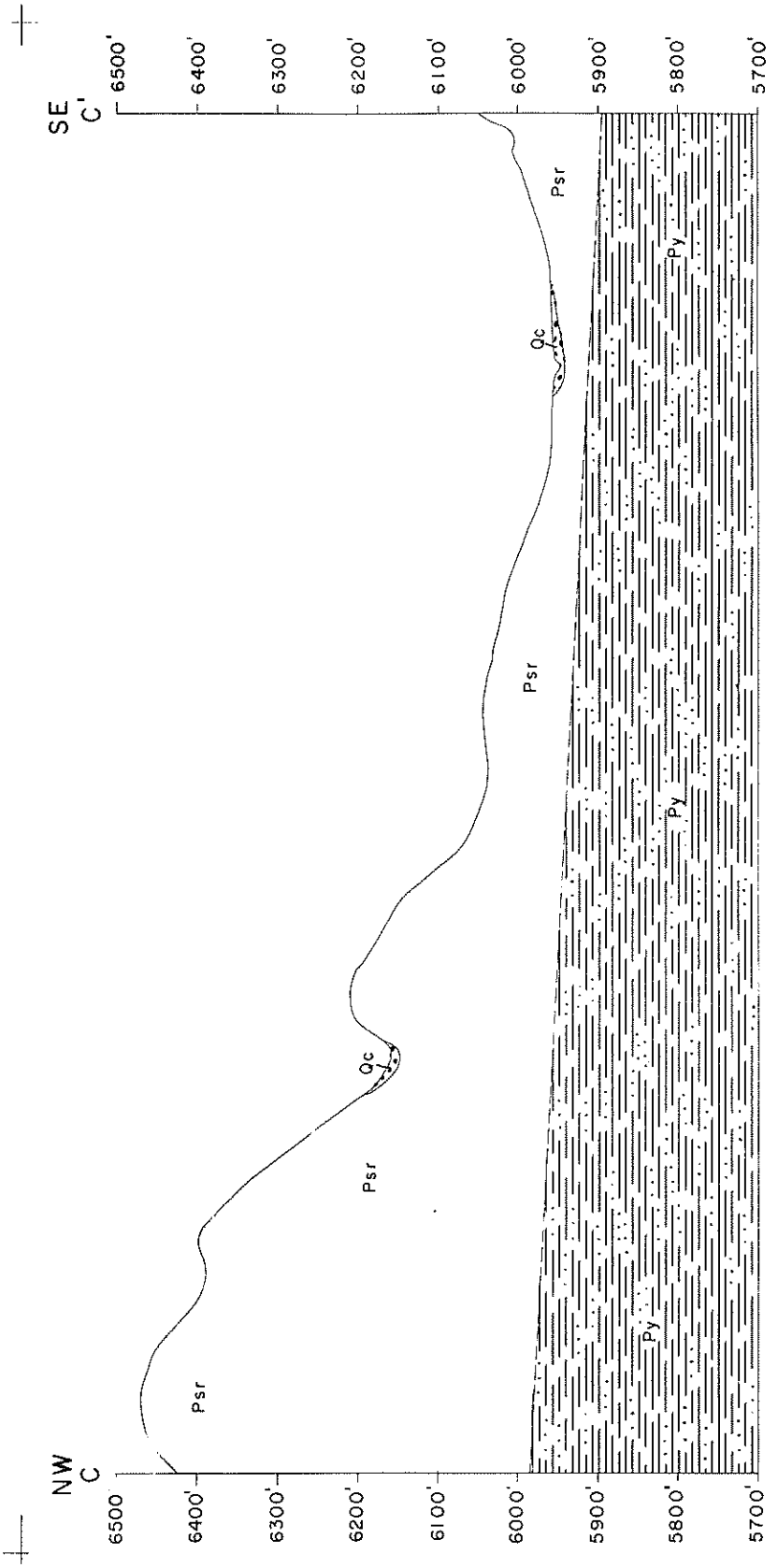

FIGURE 8 — GEOLOGIC CROSS SECTION C – C'

but the age is given as Recent because it is still forming at present. This is evidenced not only by tufa deposited at the mouth of the spring but also by calcium carbonate which was deposited on the weir used to monitor the springflow.

Colluvium Unit

This unconsolidated talus slope deposit consists of locally derived material mostly from the San Andres Formation and to a lesser degree from the Yeso Formation. It commonly contains unsorted limestone fragments of pebble to boulder size covered by a thin soil layer.

Alluvium Units

The alluvium in this area was divided into two sub-units. The first sub-unit is made up of the alluvium deposited in the Rio Peñasco flood plain. It consists mainly of fine silts and clays with some well rounded limestone fragments which range in size from coarse sand to cobbles. The second sub-unit is made up mostly of locally derived subangular to subrounded limestone fragments of pebble to boulder size with some sands, silts, and clays. This sub-unit is found in Paul and Short Canyons.

Structure

As mentioned before, this area lies on the eastern dipslope of the Sacramento uplift (Kelley, 1971). More locally it is in the central portion of the Dunken uplift which is an area of several nearly north-south trending synclines and anticlines (Kelley, 1971).

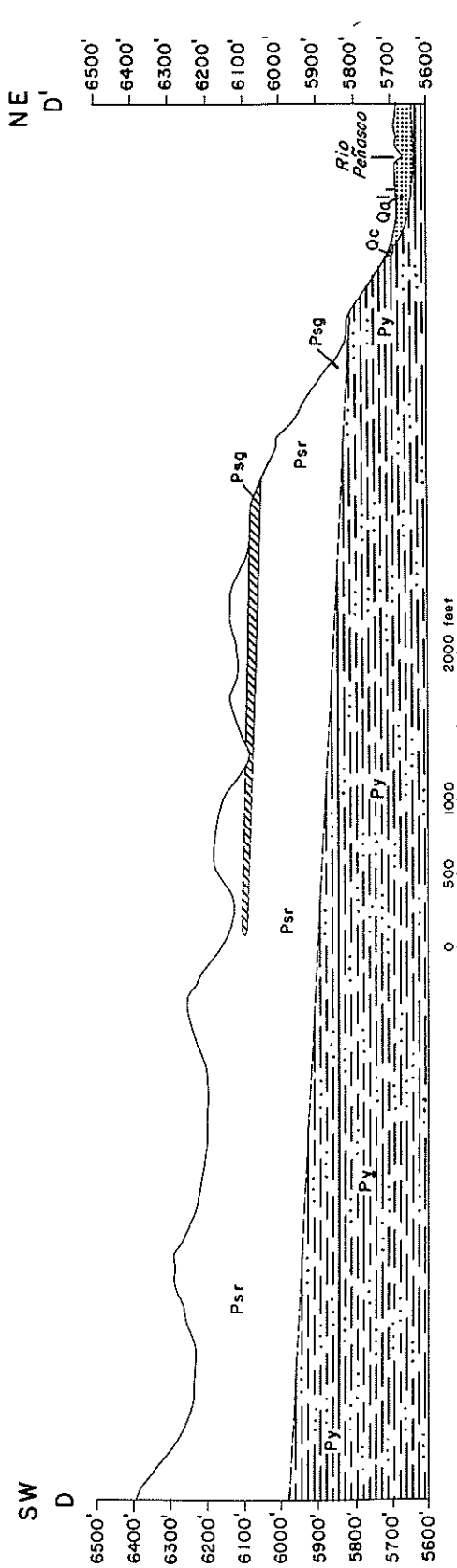

FIGURE 9 — GEOLOGIC CROSS SECTION D – D'

The study area itself is characterized by lack of any major structures. Beds within it generally dip gently toward the east (Figs. 7 and 8). The main exceptions are the beds near the contact of the Yeso and San Andres Formations. These beds generally dip in toward the hill at angles ranging from 7 to 45 degrees. Since the Yeso-San Andres contact throughout the region also dips gently toward the east, it is assumed that the bedding attitude near the contact is the result of collapse. This collapse is assumed to be due to dissolution of gypsum in the upper part of the Yeso Formation. Cross sections shown in Fig. 7 indicate this relationship. It is thought that collapse has occurred along most of the Yeso-San Andres contact but it is not shown on the cross sections due to lack of evidence. These collapse and solution features probably act to channel the ground water toward Paul Spring.

Table III. Simplified Stratigraphic Column for the Roswell Basin and the Paul Spring Area.

AGE	GROUPS, FORMATIONS, MEMBERS	DESCRIPTION
Holocene and Pleistocene	Alluvium	Predominantly fine-grained flood plain deposit of Rio Peñasco. Coarse deposits in Paul Canyon and Short Canyon.
	Colluvium Unit	Talus slope deposit mostly derived from San Andres Limestone.
	Solution Breccia Unit	Angular fragments of limestone and tufa in a calcite-cemented matrix of smaller limestone particles.
	Conglomerate Unit	Limestone fragments in a fine-grained sandy matrix, moderately cemented by caliche.
Pleistocene and Pliocene	Gatuna Formation	0-250 ft. thick. Sands, clays, gravels, red color, thin layers of carbonates.
Permian	Artesia group Tansill formation Yates formation Seven Rivers formation Queen formation Grayburg formation	0-400 ft. thick. Upper portion: Clays, sands, evaporites. Lower portion: Clays, sands, carbonates. The Queen formation is usually considered to form the aquitard.
	San Andres formation Fourmile Draw member Bonney Canyon member Rio Bonito member	200-? ft. thick. Upper portion: Evaporites, sands (Lovington sandstone), carbonates. Lower portion: Carbonates, sands (Glorieta sandstone), shales.
	Yeso formation	
Precambrian		

THE PERCHED SYSTEM

Paul Spring was chosen for this recharge study because the aquifer contributing to it is perched and considered to be small in areal extent. This is important in that it should be possible to isolate this system and obtain accurate values for the percentage of rainfall which becomes recharge.

A perched groundwater body is held above the regional water table by a layer of impermeable or semi-permeable rock. In the Paul Spring area it is difficult to show the existence of a true regional water table due to the highly variable nature of the beds which make up the Yeso Formation. Renick (1926) and Fiedler and Nye (1933) all reported that the regional water table was 500 to 1000 feet below the land surface. Appendix A gives well log data for the area around Paul Spring. These data show water being encountered at several different levels in this region. It appears that there are numerous perched water bodies at various levels, with the one contributing to Paul Spring having the highest elevation.

In order to determine the percentage of rainfall which actually enters the ground and becomes recharge water, it was necessary to delineate the boundaries of the perched system. As previously noted, the base of the aquifer is in the uppermost part of the Yeso Formation.

An examination of the geologic map (Fig. 6) and of the cross sections (Figs. 7, 8, 9) indicates that the general dip is about 3° due east or southeast in the study area. On all sides but the

southwest, the aquifer is isolated by channels that cut down to somewhat below the top of the Yeso Formation. Only the southwest side, or base, is connected to the main body of the Permian complex (Fig. 9). Lateral influx of surface water or shallow groundwater could come through this base (Fig. 10), but seems to be precluded by the general dip. A contribution from outside the recharge area seems possible only through the Yeso Formation. Solution channels and collapse features could be locally more important than the general dip in funneling lateral groundwater flow into the Paul Spring area and in controlling the point or points of discharge. The Yeso outcrops south of Paul Spring show no evidence of appreciable groundwater discharge taking place at present.* A denser vegetation, mostly of juniper trees, characterizes the slopes just below the Yeso/San Andres contact. It is probably due to greater moisture retention by the semipermeable layer rather than to lateral groundwater movement.

The recharge area, outlined in Fig. 10, follows the exposed contact between the Yeso and San Andres formations; it includes a narrow zone beyond the exposed contact that could provide water for Paul Spring through channeling. The total recharge area was measured with a planimeter and found to be 14,160,438 square feet.

* A patch of solution breccia in Short Canyon (Fig. 6) indicates that other springs existed in the recent past.

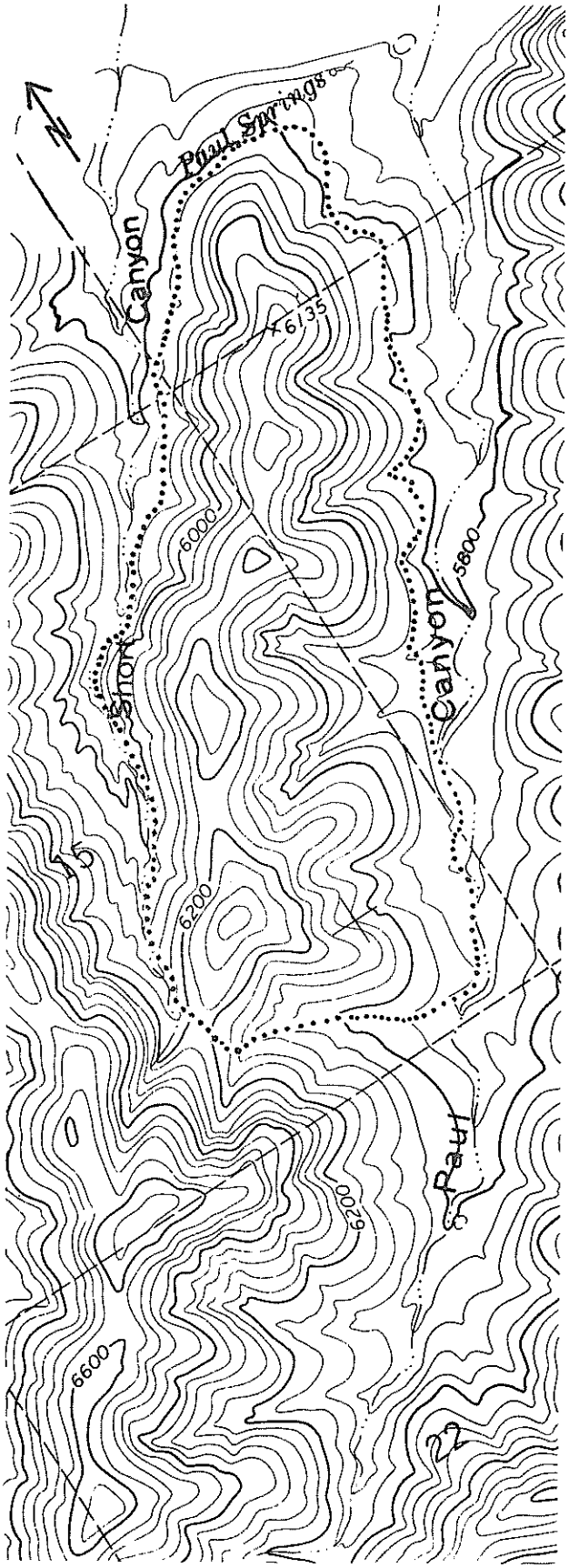

Fig. 10. Recharge area contributing to the Paul Spring aquifer.

TRITIUM IN PRECIPITATION AND SPRING WATER

Water samples from Paul Spring, collected since 1973, and precipitation samples from Elk have been analyzed for natural tritium.

Tritium has a known half-life of 12.36 years. Therefore, using the available data it should be possible to calculate the flow velocity and the age of the ground water issuing from Paul Spring. These parameters are of particular importance because they could provide an estimate of the delay between recharge and discharge and also provide additional information about the perched system.

The tritium content is reported in tritium units (TU) defined as

1 TU = 1 tritium atom per 10^{18} hydrogen atoms.

Tritium values for the area of interest are given in Tables IV and V. A graph of spring flow and precipitation tritium activity versus time is given in Fig. 11. It should be noted that every precipitation event is not represented. This is either because a sample was not collected or several events were lumped together to obtain enough water for tritium analysis. On examination of this plot it is evident that the relationship between tritium in precipitation and tritium in springflow is quite complex. Possible correlations of peaks yield travel times that range from 150 to 500 days but the validity of these values is questionable.

The actual amount of tritium entering the ground water system may have more effect on the tritium content of the spring water

Table IV. Tritium in Precipitation at Elk.

Date	Amount of Precipitation (in.)	TU
07/74	.44	49.6
08/74	5.44	49.2
08/24-30/74	4.25	39.4
09/74	10.03	33.7
03/12+30/75	.54	97.2
05/11-30/75	.39	68.3
07/03-10/75	1.11	55.8
07/11/75	1.65	68.4
07/12-27,29,30/75	1.94	56.3
08-09/75	5.46	24.5
06/76	1.22	58.2
07/76	3.28	24.1
11/12,28/76	.94	30.7
02/15/77	1.20	45.2
04/14/77	1.49	42.5
05/08/77	1.57	44.5
05/22/77	1.12	54.4
06/15/77	1.38	76.3
08/11/77	2.30	26.5
09/07/77	1.33	31.1
10/3,6/77	.50	20.7

than the relative concentration of tritium in precipitation. For example, a small precipitation event with a high tritium content may cause less fluctuation in spring water tritium than a large precipitation event with relatively low tritium concentration. Therefore, individual precipitation amounts were multiplied by their corresponding tritium concentrations. These values were then plotted and compared to tritium measurements of spring water (Fig. 12). As in Fig. 11, the graphs in Fig. 12 do not show any obvious correlation.

Even though there is a lack of correlation in Figs. 11 and 12, they indicate several important features about the flow system. The fact that the plots do not correlate is evidence that the perched aquifer is a complicated system. Geologic reasons for this complexity include the collapse features of the upper Yeso Formation and the existence of the Glorieta Sandstone in the recharge area. The collapse features probably cause the ground water flow paths to be highly irregular in direction and length. This would serve to mask the effect of a tritium peak in precipitation which recharges the aquifer. As discussed below (p.89), the Glorieta Sandstone acts as a filter and dampens the aquifer response to percolation.

The tritium values for springflow in Figs. 11 and 12 are an important indication of flow conditions in the Paul Spring aquifer. When considering the tritium input, that is tritium in precipitation, these measurements indicate long travel times and relatively old ground water. This would not be expected for such a small

Table V. Tritium in Water from Paul Spring.

Date	TU	Date	TU
07-11-73	20.0	02-19-77	14.1
04-08-74	10.1	05-05-77	3.5
06-15-74	10.4	06-30-77	1.6
08-23-74	13.8	07-15-77	1.5
12-19-74	1.7	08-17-77	12.1
02-21-75	1.5	09-16-77	5.5
08-28-75	13.0	10-07-77	2.1
12-19-75	5.3	10-22-77	1.9
03-27-76	10.8	11-19-77	1.4
06-05-76	5.1	12-16-77	2.3
08-10-76	10.4	01-14-78	0.9
12-03-76	9.4	02-11-78	2.5
12-22-76	7.4	03-11-78	1.8
01-04-77	2.5	04-02-78	2.0
01-29-77	3.7		

system. An apparent age can be obtained by taking a weighted average of tritium concentration in precipitation and comparing it to the average tritium value for spring flow. The formula for the weighted average is given as

$$T_{pa} = \frac{\sum_{i=1}^{n} T_{pi} \times p_i}{\sum p_i} \qquad (1)$$

where

T_{pa} = average tritium content of precipitation

T_{pi} = Tritium content of the i^{th} precipitation sample

p_i = amount of precipitation contributing to the i^{th} sample

n = number of samples.

Using Eq. (1) we obtain an average tritium content in precipitation of 40.7 TU. The average tritium value of spring flow is 7.5 TU.

For a first approximation of the apparent age of the ground water, a piston type flow equation is used (Nir, 1964). This equation is of the form:

$$C = C_o e^{-t/t_m} \qquad (2)$$

where

C = concentration of tritium in the spring water

C_o = concentration of tritium in the precipitation

t_m = mean life of tritium, 17.8 years

t = time in years

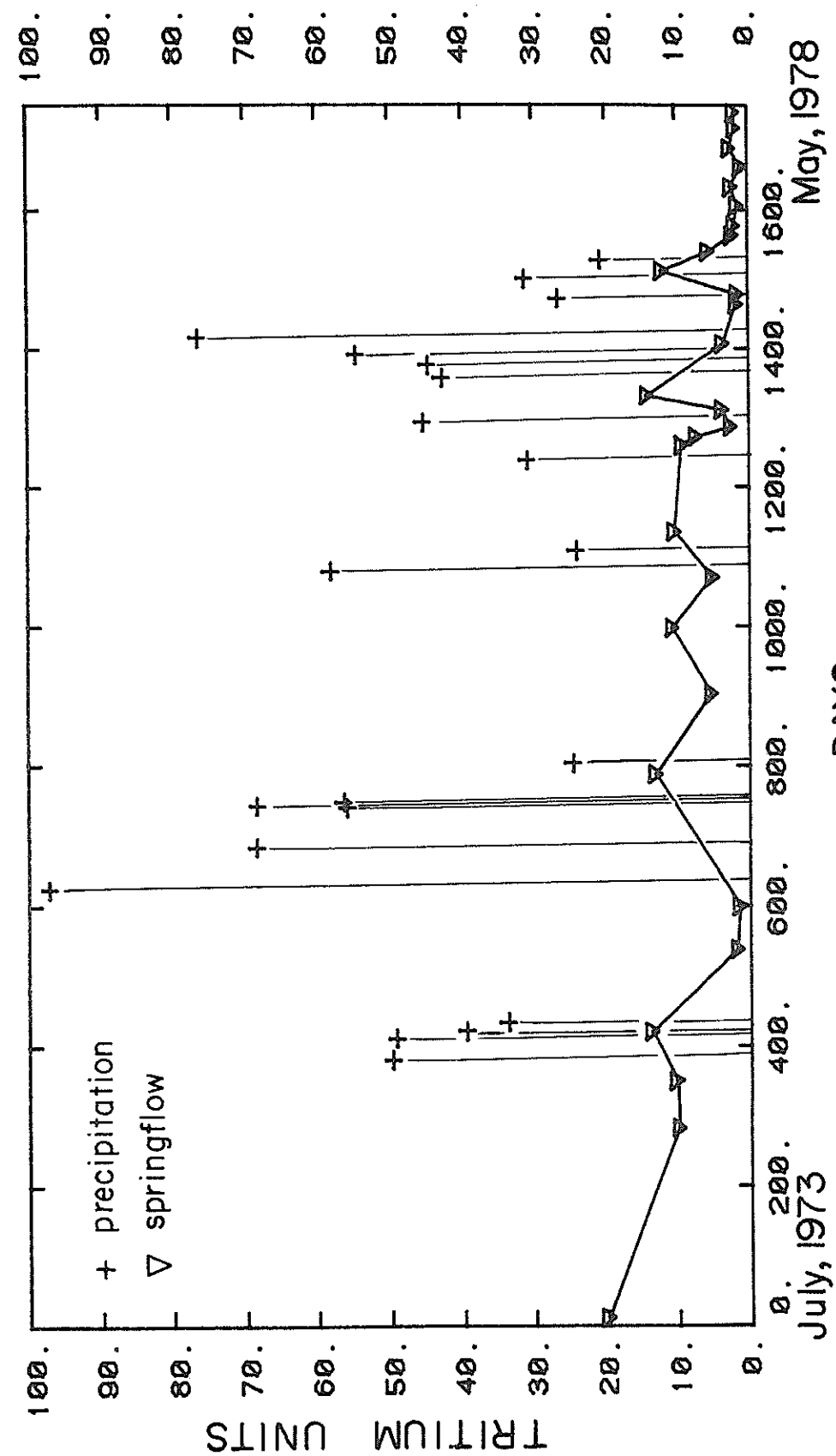

Fig. 11. Tritium activity in springflow and precipitation at Paul Spring (Elk precipitation records).

Solving Eq. (2) for t yields

$$t = -t_m \ln \frac{C}{C_o}$$

which leads to a value of 30.4 years for the apparent age of the ground water in the Paul Spring aquifer. This appears to be quite old for such a small system.

To take into account the effects of dispersion, an equation for a laminar flow dispersive system is used (Nir, 1964). This equation is given as

$$C = C_o(4\tau + 1)^{-\frac{1}{2}} \exp\{\frac{t^*}{2\tau} (1 - (4\tau + 1)^{\frac{1}{2}})\} \qquad (3)$$

where

$$\tau = \frac{D_m}{v\ t_m}$$

D_m = dispersion coefficient

v = velocity

$t^* = t/t_m$

Solving for t in Eq. (3) gives

$$t = \frac{t_m 2\tau \log_e [C/C_o(4\tau + 1)^{\frac{1}{2}}]}{1 - (4\tau + 1)^{\frac{1}{2}}}$$

According to Nir (1964), a realistic value for τ is about 0.1. Using that value we obtain an apparent age of the Paul Spring water of 29.9 years, close to the value computed above. An age of 30 years seems unlikely if all or most of the water is derived from local infiltration. The water would predate the atmospheric nuclear tests of the fifties and early sixties and this is contradicted by

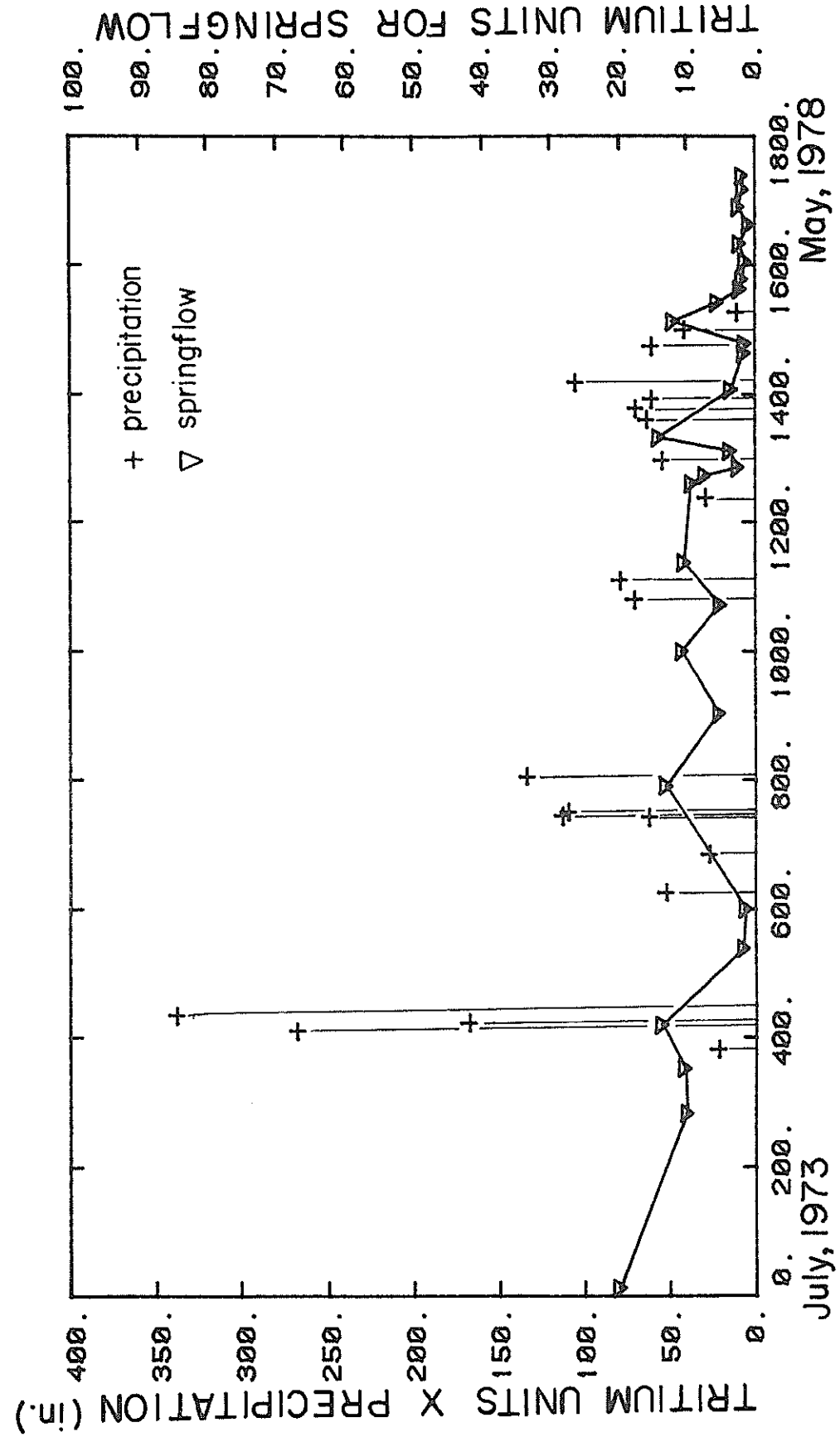

Fig. 12. Comparison of tritium activity in Paul Spring discharge with weighted tritium activity in precipitation.

the occasional post-bomb tritium values that have been measured. They indicate admixture of relatively young water. This would also account for the lack of correlation between tritium in precipitation and tritium in springflow records. The geology of the Paul Spring perched system makes this interpretation plausible. The spring issues from a point very near the Yeso-San Andres contact. If water flowed laterally through the silts of the upper Yeso Formation it would probably travel very slowly whereas water flowing mostly through the limestones of the lower San Andres Formation would travel relatively much faster. These two sources for the groundwater must be considered. Thus, if the head is low (i.e. low flow) a relatively larger amount of water should be coming from the silts of the upper Yeso Formation. When the head is higher, relatively more spring water should be derived from the lower San Andres Formation. To investigate this, tritium values of springflow are plotted in Fig. 13 along with the discharge at the time the tritium samples were taken. This plot shows a delayed relationship between increased flow and "younger" waters. When the flow increases it has a piston effect and pushes out "older" waters which are then followed by the relatively "younger" waters.

Since so much "older" water appears to be contained in the upper Yeso Formation there cannot be a large amount of vertical movement of water through this formation. If the vertical movement was much greater, the downward flowing "younger" waters would tend to

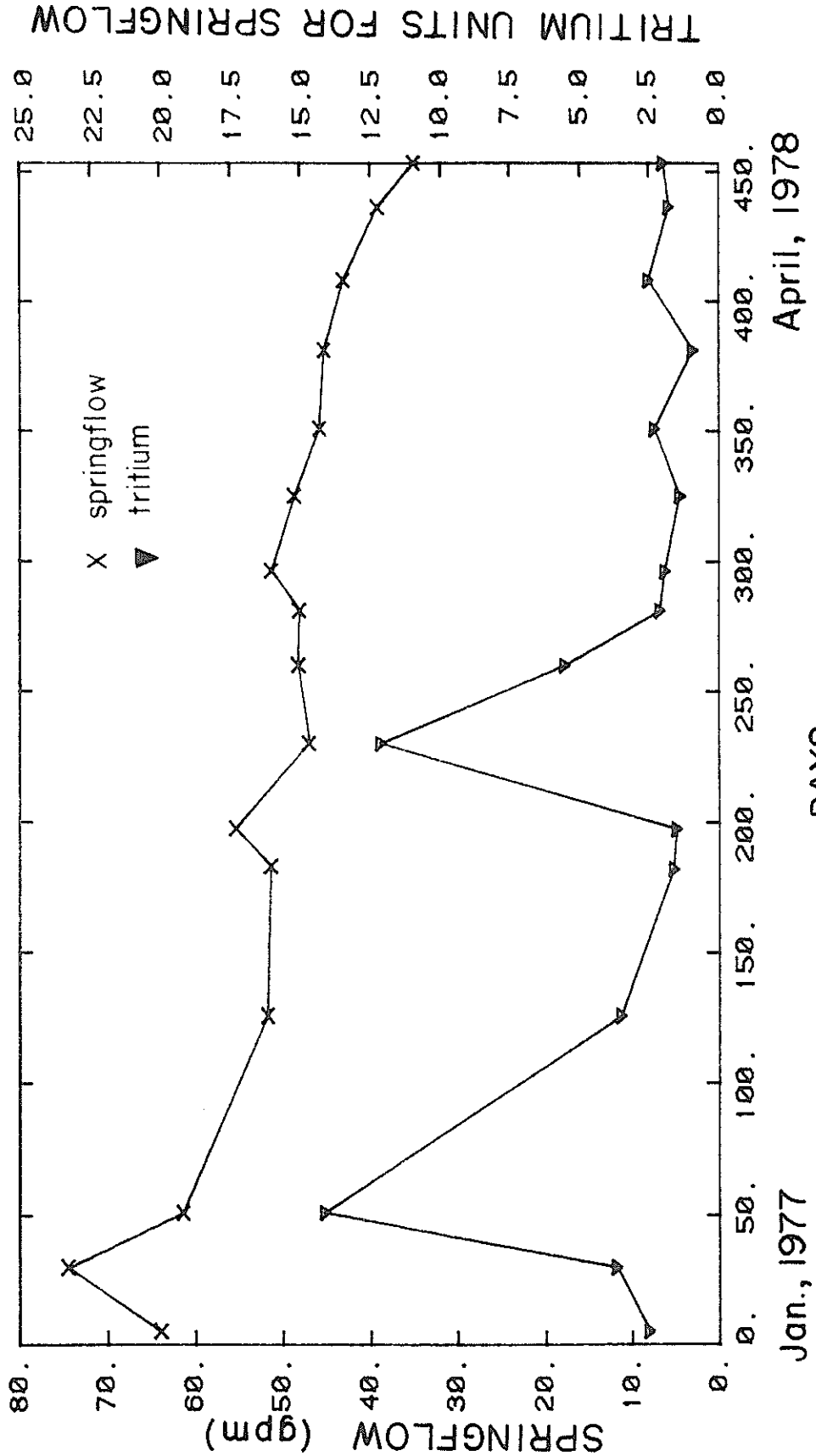

Fig. 15. Paul Spring discharge. Comparison of tritium activity with discharge volume.

flush out these "older" waters. A low vertical flow rate through the base of the perched system should be expected.

The mean tritium contents of precipitation and spring water can be used to estimate a mixing ratio

$$R_m = \frac{Q_p}{Q_p + Q_u} = \frac{7.5}{40.5} = 0.184$$

where Q_p = spring discharge derived from precipitation;

Q_u = spring discharge derived from underflow.

This estimate (and it is only an estimate) indicates that only about 18% of the springflow should be used to compute a recharge fraction.

SPRINGFLOW MEASUREMENTS

The flow of Paul Spring was continuously recorded for 453 days, from January 4, 1977 to April 1, 1978. The techniques are described in Appendix B. Numerical data for daily average springflow are tabulated in Appendix C.

A graph of springflow vs. time is given in Fig. 14. Springflow is corrected for diversion, leakage and clogging of the V-notch and stilling well by debris (Appendix B). Short-term fluctuations of springflow are superposed on a monotonic decline over the whole time span of measurement.

The short-term declines were interpreted as recession curves from individual or closely spaced rainfall events. A number of these were selected for recession curve analysis. They are listed in Appendix D.

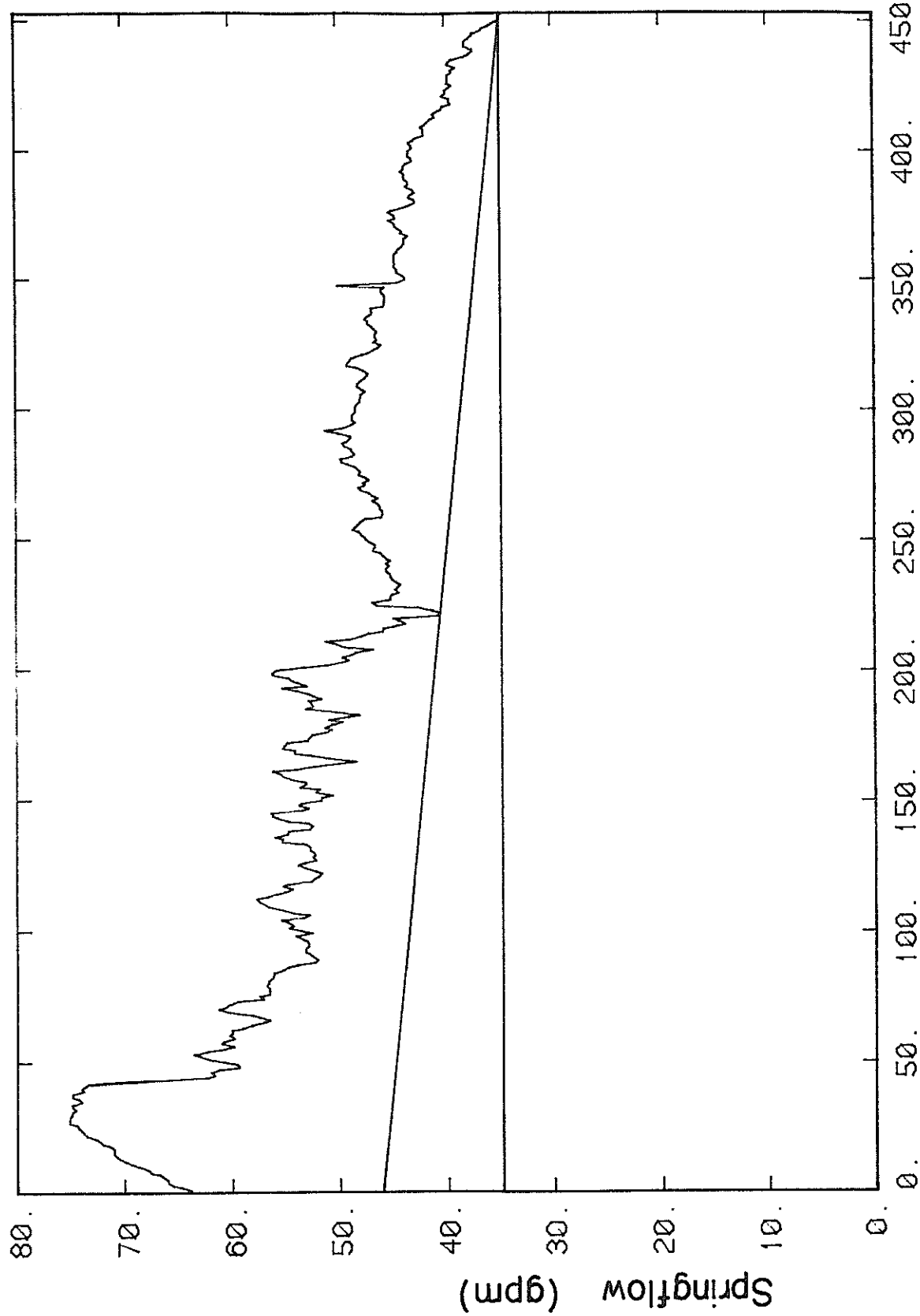

Fig. 14. Springflow vs. time. The straight lines represent two possible deep flow components.

RECHARGE ESTIMATES AT PAUL SPRING

Approach

In order to estimate the amount and percentage of precipitation which becomes recharge it is necessary to formulate a governing equation which utilizes the available data. For the Paul Spring area these data consist of daily precipitation records over a period of many years and springflow measurements of 453 days. Since there is no information on how the parameters of the Paul Spring aquifer vary in space, i.e. wells or other springs, it is necessary to use a lumped parameter approach. In this model the aquifer is thought of as a phreatic linear reservoir in which the spatial variations of the water level fluctuations are averaged (Fig. 15).

A water balance for this system can then be written in the form

$$S_y \frac{dh}{dt} + a(h-h_o) = \varepsilon'$$

where

S_y = average storage coefficient (specific yield of the phreatic aquifer), a dimensionless constant

h = average water table height [L]

h_o = level at which the outflow is zero [L], taken to be constant

a = outflow constant [T^{-1}]

ε' = recharge rate [L/T]

t = time

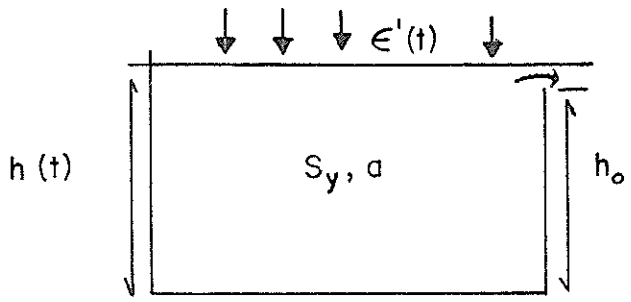

Fig. 15. The phreatic linear reservoir.

The outflow is then approximated by:

$$q = a(h - h_o) \tag{5}$$

where q = outflow per unit area [L/T]

To obtain an equation in terms of the total inflow and outflow we first multiply Eq. (4) by the total area of the aquifer, A. This gives

$$S_y A\frac{dh}{dt} + Aa(h - h_o) = A\varepsilon' \tag{6}$$

The term $Aa(h - h_o)$ can now be written as:

$$Aa(h - h_o) = qA = Q \tag{7}$$

where Q = total outflow [L^3/T]

The recharge term can then be approximated as a linear function of the precipitation, as follows:

$$\varepsilon' = rp \tag{8}$$

where

r = the fraction of precipitation which becomes recharge, a dimensionless constant.

p = precipitation [L/T]

Solving for h in terms of Q gives:

$$h = Q/Aa + h_o \tag{9}$$

Substituting Eqs. (7), (8), and (9) into Eq. (6) yields

$$S_y A\frac{d(Q/Aa + h_o)}{dt} + Q = Arp \tag{10}$$

or

$$\frac{S_y}{a}\frac{dQ}{dt} + Q = Arp. \tag{11}$$

Eq. (11) relates the spring flow, Q, to the precipitation, p.

The following calculations are based on this model. We will use both numerical methods and a stochastic approach.

Tritium measurements suggest that the Paul Spring discharge consists of a mixture of water derived from local precipitation and water transmitted through the Yeso Formation. Therefore we will test three hypotheses:

(1) All springflow is derived from precipitation falling on the spring's recharge area.

(2) Recharge by precipitation is superposed on a steady component of deep flow (34.8 gpm).

(3) Recharge by precipitation is superposed on a deep-flow component linearly decreasing from 46.4 gpm to 34.8 gpm over the duration of the springflow measurements (453 days).

Recession Curve Analysis and Numerical Methods

If we define the right-hand side of Eq. (11) as the net recharge R, we can write

$$\frac{S_y}{a} \frac{dQ}{dt} + Q = R \tag{12}$$

where

$$R = Arp.$$

Now define a spring flow recession as a downward trend in the spring discharge due to the absence of recharge. Then, during periods of spring flow recession we can write Eq. (12) as

$$\frac{S_y}{a} \frac{dQ}{dt} + Q = 0. \tag{13}$$

The solution to Eq. (13) is easily shown to be

$$Q = \hat{Q}\, e^{-\frac{a}{S_y} t}\ , \tag{14}$$

where $\hat{Q}$ is the initial flow of the recession period. The springflow record contains numerous recharge/recession events ranging from 1 to 10 days in length. A list of the dates of the spring flow recessions is given in Appendix D. For each separate recession period, the initial flow is $\hat{Q}$. Each subsequent data point of the period was divided by $\hat{Q}$. Each recession period was therefore normalized on a scale of 0 to 1.

Eq. (14) can now be written in finite difference form and rearranged to yield

$$\left(\frac{a}{S_y}\right)_k^{(\ell)} = \frac{-\log_e(Q_k^{(\ell)}/\hat{Q}^{(\ell)})}{\Delta t} \; ; \; k = 1, b; \; \ell = 1, c \qquad (15)$$

where b = number of points in the ℓ^{th} recession period,

c = number of recession periods.

Eq. (15) is solved to yield b x c values of a/S_y. The computer program used, along with each value of S_y/a is given in Appendix D. An average value of a/S_y is obtained, the inverse of which is the desired model parameter S_y/a. In the above manner, the hydraulic response time of the system S_y/a , was found to be 48.4 days.

Method 1: Recharge estimation using Simpson's rule

In order to provide a check of the results, two methods were used to solve for the net recharge, R. The first method follows much the same procedure for calculating net recharge as was used by Updegraff and Gelhar (1977) for the Mesilla Valley.

Eq. (12) is integrated over two time intervals using Simpson's Rule to yield

$$\int_{j-1}^{j+1} \frac{S_y}{a} \frac{dQ}{dt} \, dt + \int_{j-1}^{j+1} Q dt = \int_{j-1}^{j+1} R dt \; , \qquad (16)$$

or written in finite difference form

$$\frac{3}{\Delta t} \frac{S_y}{a} (Q_{j+1} - Q_{j-1}) + (Q_{j+1} + 4Q_j + Q_{j-1}) = (R_{j+1} + 4R_j + R_{j-1}). \qquad (17)$$

Eq. (17) will produce n equations with n+2 unknowns, where n equals the total number of days of record. The left-hand side of Eq. (17) is known for every point, j, where j ranges from 2 to n-1, and we can

determine the left-hand side at j=1 and j=n if we estimate a value for Q_o and Q_{n+1}. These values, obtained by extrapolating the spring flow record linearly one day, are 63.0 gpm and 34.8 gpm, respectively. Setting the left-hand side of Eq. (17) equal to a variable A_j, where j ranges from 1 to n, and writing the resulting set of equations in matrix form we obtain

$$\begin{bmatrix} R_o + 4R_1 + R_2 \\ R_1 + 4R_2 + R_3 \\ \vdots \\ R_{n-1} + 4R_n + R_{n+1} \end{bmatrix} = \begin{bmatrix} A_1 \\ A_2 \\ \vdots \\ A_n \end{bmatrix} \qquad (18)$$

The system of Eqs. (15) is easily solved using the Thomas algorithm if we write the R matrix in tridiagonal form as

$$\begin{bmatrix} 4R_1 + R_2 \\ R_1 + 4R_2 + R_3 \\ \vdots \\ R_{n-1} + 4R_n \end{bmatrix} = \begin{bmatrix} A_1 - R_o \\ A_2 \\ \vdots \\ A_n - R_{n+1} \end{bmatrix} \qquad (19)$$

where R_o and R_{n+1} are estimated by

$$R_o = \frac{S_y}{a} \frac{Q_1 - Q_o}{\Delta t} + Q_1 \ ,$$

$$R_{n+1} = \frac{S_y}{a} \frac{Q_{n+1} - Q_n}{\Delta t} + Q_n \ .$$

We now have n equations with n unknowns and can solve for the daily net recharge R_j corresponding to the daily spring flow Q_j. The

results of method 1, along with the results of the following method 2, are plotted in Fig. 16. Listings of the computer programs and numerical results are given in Appendix E.

Method 2: Recharge estimation using finite difference approximation

Method 2 is easier and shorter than method 1 and will be shown to yield essentially the same results. In method 2, Eq. (12) is written in finite difference form as

$$\frac{S_y}{a}\frac{1}{2\Delta t}(Q_{j+1} - Q_{j-1}) + Q_j = R_j \ , \qquad (20)$$

where

$$R_1 = \frac{S_y}{a}\frac{1}{2\Delta t}(Q_2 - Q_o) + Q_1 \ ,$$

$$R_n = \frac{S_y}{a}\frac{1}{2\Delta t}(Q_{n+1} - Q_{n-1}) + Q_n \ .$$

The daily net recharge calculated using method 2 is plotted in Fig. 16 (bottom). From a visual inspection of the figure, we can see that both methods yield about the same results. The similarity is also demonstrated by comparing the total net recharge of each method.

METHOD	TOTAL NET RECHARGE
1 - Simpson's Rule	4.17287×10^6 ft^3
2 - Finite Difference	4.17531×10^6 ft^3

The results differ by less than .1%.

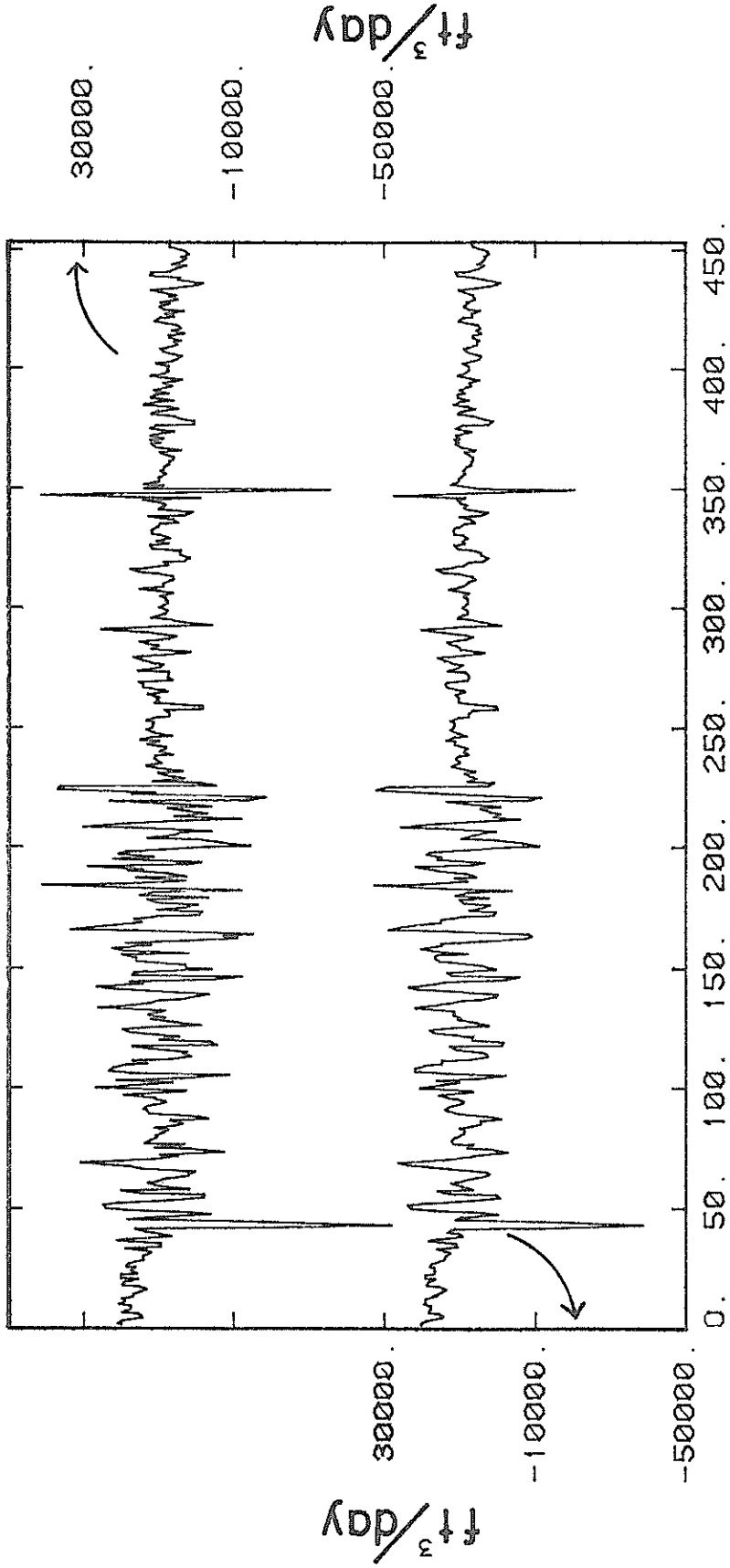

Fig. 16. Recharge estimates by Simpson's rule (top-right scale) and by finite differences (bottom-left scale).

We can also calculate the total change in storage by subtracting the total spring flow from the average total recharge calculated from methods 1 and 2.

Average Total Recharge	4.17×10^6 ft^3
Total Spring Flow	-4.44×10^6 ft^3
Total Loss From Storage	$- .27 \times 10^6$ ft^3

Calculation of the Percentage of Precipitation that Becomes Recharge

First, we return to our original definition of net recharge

$$R = Arp \ , \tag{21}$$

where R = volume of recharge

A = area where recharge occurs

r = percentage of precipitation that becomes recharge

p = precipitation (depth over the surface in feet).

We can solve for the percentage of precipitation that becomes recharge by rearranging terms in Eq. (21) to yield

$$r = \frac{R}{Ap} = \frac{\text{Total Recharge}}{\text{Total Volume of Precipitation}}$$

We must now determine which period of precipitation corresponds to the observed spring flow and recharge. Precipitation is unlikely to cause an immediate fluctuation in the water table elevation, and therefore an increase in spring flow. The physical situation would indicate that there must be a delay between the time the precipitation event occurs and the time the spring flow increases.

Basically the time delay is the sum of two processes.

First, the water must infiltrate from the ground surface down to the water table, and, second, the system must respond to the increase in hydraulic head. Therefore we will assume the observed springflow originated as precipitation that fell at an earlier time.

We attempted to determine the precipitation lag time using a statistical measure called the cross covariance. The cross covariance function is

$$\gamma_{xy} = E\{[x(t) - \mu_x][y(t+u) - \mu_y]\}$$

where $E\{\}$ = expected value

$x(t)$ = value of the x series at time t

$y(t+u)$ = value of the y series at u time counts from t (u can be positive or negative)

μ_x = mean value of the x series

μ_y = mean value of the y series .

The function has a maximum value when peaks and troughs of the $x(t)$ series match peaks and troughs of the $y(t+u)$ series. A computer program developed by A. Gutjahr and C. Mumma of New Mexico Institute of Mining and Technology was used. We examined the cross covariance between (1) daily recharge and daily precipitation; (2) the 20-day moving average of recharge and the 20-day moving average of precipitation; (3) daily springflow and daily precipitation. A 20-day moving average is performed by averaging the value at time t with the 19 preceding time periods. The first 19

Table VI. Cross-Covariance Peaks

Spring Flow vs. Precipitation	
43 days	0.41354×10^{-4} cm^2
97 days	0.58286×10^{-4} cm^2
152 days	0.96933×10^{-4} cm^2
191 days	1.04766×10^{-4} cm^2
277 days	0.18384×10^{-4} cm^2
360 days	0.11099×10^{-4} cm^2

Recharge vs. Precipitation (20 day moving average)	
6 days	0.09940×10^{-4} cm^2
30 days	0.07545×10^{-4} cm^2
66 days	0.69920×10^{-4} cm^2
136 days	1.69838×10^{-4} cm^2
179 days	1.46615×10^{-4} cm^2
224 days	0.02316×10^{-4} cm^2

(Most likely range: 120-200 days)

days of record are lost in this averaging process.

We had hoped to find a single peak in the cross covariance at some lag time, but instead found multiple peaks at a variety of lag times (Table VI). The daily recharge and precipitation cross covariance contained so many peaks that the function amounted to little more than noise. We were unable to determine a lag time based on the present data. The 20-day moving average was a first attempt at accounting for the filtering effect of percolation through the unsaturated zone. It produced 6 peaks, the maximum occurring at 136 days.

The lag time is a significant factor in determining the recharge percentage because the period of springflow record coincided with a period of diminished precipitation. Precipitation was generally greater prior to the 453 days of springflow record. Therefore, the longer the lag time the smaller the recharge percentage. This can be appreciated from Fig. 17 where springflow is lagged against precipitation at 50-day intervals. Recharge percentages computed from these lagged records are shown in Table VII.

The cross covariance between springflow and precipitation had a maximum at 191 days. The physical significance is uncertain since recharge is really the correlatable parameter. The recharge/precipitation function can be strongly nonlinear. Moreover, a lag time of 191 days is much greater than the response time (48 days) computed from recession curve analysis. Nonetheless, we include a recharge estimate based on this correlation because, as mentioned above, a maximum was not obtained with the recharge/springflow correlation.

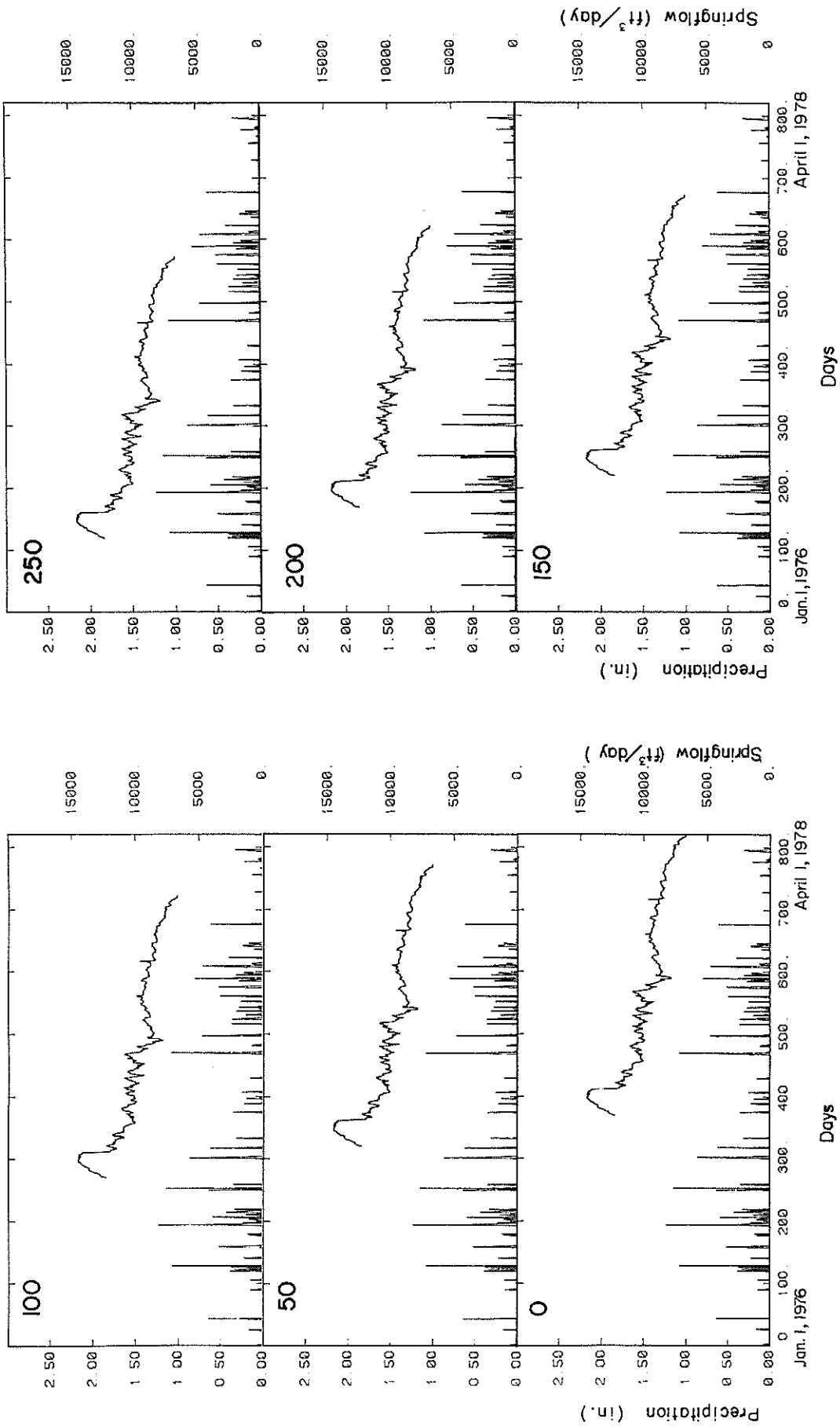

Fig. 17. Springflow lagged against precipitation by the number of days indicated on top left corner of each graph.

A plot of the springflow and of the precipitation that occurred 191 days before, as a function of time, is given in Fig. 18.

Total precipitation, $p = 1.6109$ ft

Total volume of precipitation, $A \times p = 2.28 \times 10^7$ ft^3

Total springflow, $R = 4.17 \times 10^6$ ft^3 .

$$r = \frac{R}{Ap} = \frac{4.17 \times 10^6 \text{ ft}^3}{2.28 \times 10^7 \text{ ft}^3} \times 100 = 18.3\%.$$

The percentage is high. It is typical of values obtained when recharge is assumed to be derived totally from local precipitation.

Table VII. Recharge Percentage as a function of lag for different deep-flow hypotheses.

Lag	No Deep Flow	Constant Deep Flow	Linear Deep Flow
0	27.7	7.6	4.9
50	28.7	7.8	5.1
100	25.1	6.9	4.5
150	22.7	6.2	4.0
200	18.1	5.0	3.2
250	18.8	5.1	3.3

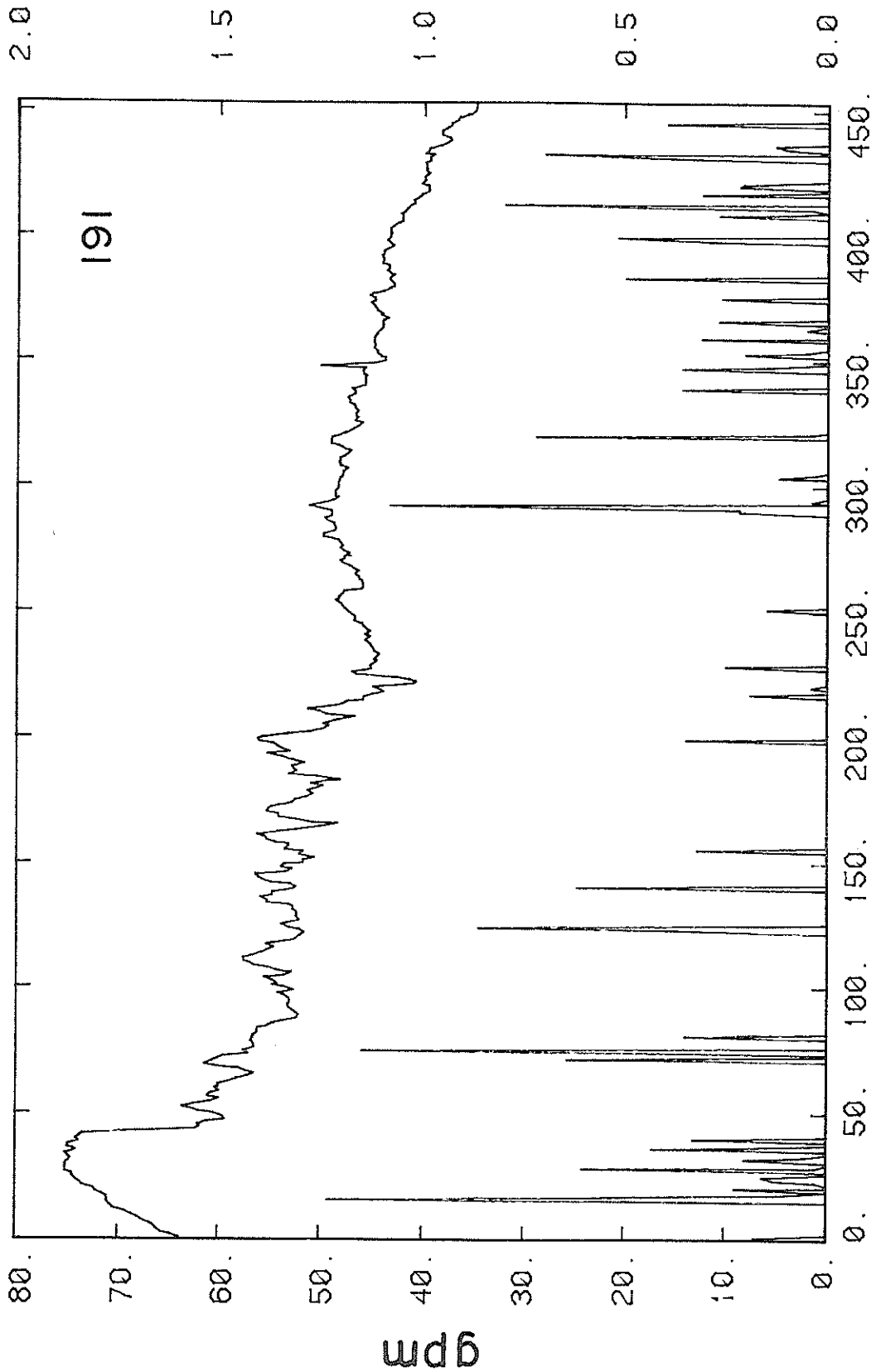

Fig. 18. Springflow lagged 191 days against precipitation.

Stochastic Approach to Recharge Estimation

In this section a stochastic approach to calculate recharge parameters is attempted. This is done to serve as a check on the previously obtained values, and to evaluate other parameters of the Paul Spring aquifer. Considering that the input to the system, precipitation, appears to be random in time, this approach should yield reasonable estimates.

The basis of this approach for a linear reservoir, lumped parameter system was presented by Gelhar (1974). Assuming that we are dealing with a stationary random process, equations will be developed which relate the input spectrum (precipitation) to the output spectrum (springflow). For complete coverage of the mathematics of this approach the reader is referred to Jenkins and Watts (1968).

The ordinary partial differential equation which governs this system was given in Eq. (11) as

$$\frac{S_y}{a}\frac{dQ}{dt} + Q = Arp$$

We now let $Ap = \varepsilon$ and Eq. (11) becomes

$$\frac{S_y}{a}\frac{dQ}{dt} + Q = r\varepsilon \tag{22}$$

S_y and $\underline{a}$ are taken to be constants with $\underline{Q}$ and $\underline{\varepsilon}$ being stationary random functions of time. Following Lumley and Panofsky (1964), $\underline{Q}$ and $\underline{\varepsilon}$ can be represented by Fourier-Stieltjes integrals of the form

$$Q(t) = \int_{-\infty}^{\infty} e^{i\omega t} dZ_Q(\omega) \tag{23}$$

and

$$\varepsilon(t) = \int_{-\infty}^{\infty} e^{i\omega t} dZ_{\varepsilon}(\omega) \tag{24}$$

where ω is the frequency and $dZ_Q(\omega)$ and $dZ_{\varepsilon}(\omega)$ may be thought of as the Fourier amplitudes of the process.

The processes $Z_Q(\omega)$ and $Z_{\varepsilon}(\omega)$ have "orthogonal increments" (Lumley and Panofsky, 1964), which is to say that nonoverlapping differences are not correlated:

$$\langle dZ_Q(\omega_1) dZ_Q^*(\omega_2) \rangle = \begin{cases} 0 \text{ for } \omega_1 \neq \omega_2 \\ \phi_{QQ} d\omega \text{ for } \omega_1 = \omega_2 \end{cases} \tag{25}$$

$$\langle dZ_{\varepsilon}(\omega_1) dZ_{\varepsilon}^*(\omega_2) \rangle = \begin{cases} 0 \text{ for } \omega_1 \neq \omega_2 \\ \phi_{\varepsilon\varepsilon} d\omega \text{ for } \omega_1 = \omega_2 \end{cases} \tag{26}$$

where

$*$ ≡ complex conjugate

$\langle\ \rangle$ ≡ expected value

ϕ ≡ spectral density function (spectrum).

Substituting Eqs. (23) and (24) into Eq. (22) gives

$$\frac{S_y}{a} \frac{d}{dt} \int_{-\infty}^{\infty} e^{i\omega t} dZ_Q(\omega) + \int_{-\infty}^{\infty} e^{i\omega t} dZ_Q(\omega) - r \int_{-\infty}^{\infty} e^{i\omega t} dZ_{\varepsilon}(\omega) = 0$$

which can be written as

$$\int_{-\infty}^{\infty} e^{i\omega t} \left[\left(\frac{i\omega S_y}{a} + 1 \right) dZ_Q(\omega) - r dZ_{\varepsilon}(\omega) \right] = 0$$

Since $e^{i\omega t}$ is composed of a combination of sines and cosines, the integral of $e^{i\omega t}$ must always be different from zero.

Therefore

$$\left(\frac{i\omega S_y}{a} + 1 \right) dZ_Q(\omega) = r dZ_\varepsilon(\omega) \quad . \tag{27}$$

Multiplying Eq. (27) by its complex conjugate

$$\left(\frac{-i\omega S_y}{a} + 1 \right) dZ_Q(\omega) = r dZ_\varepsilon(\omega)$$

and taking the expected value of both sides, yields

$$\left(\frac{\omega^2 S_y{}^2}{a} + 1 \right) \phi_{QQ} + r^2 \phi_{\varepsilon\varepsilon}$$

which may be written

$$\frac{\phi_{\varepsilon\varepsilon}}{\phi_{QQ}} = \frac{\omega^2 S_y{}^2}{a^2 r^2} + \frac{1}{r^2} \quad . \tag{28}$$

It should now be possible to plot the ratio of the spectrum of ε to the spectrum of Q versus the frequency squared and obtain values for $\frac{S_y}{a}$ and r (Fig. 19).

The best fit for the above linear regression was attained using weekly totaled values for the ε and Q spectrums. This produced 64 data points. Following Wastler (1969), the number of lags used was 10 percent, or 6 lags. Values obtained from a least squares linear regression are given below.

Coherence = .985

$1/r^2 = 128.48$

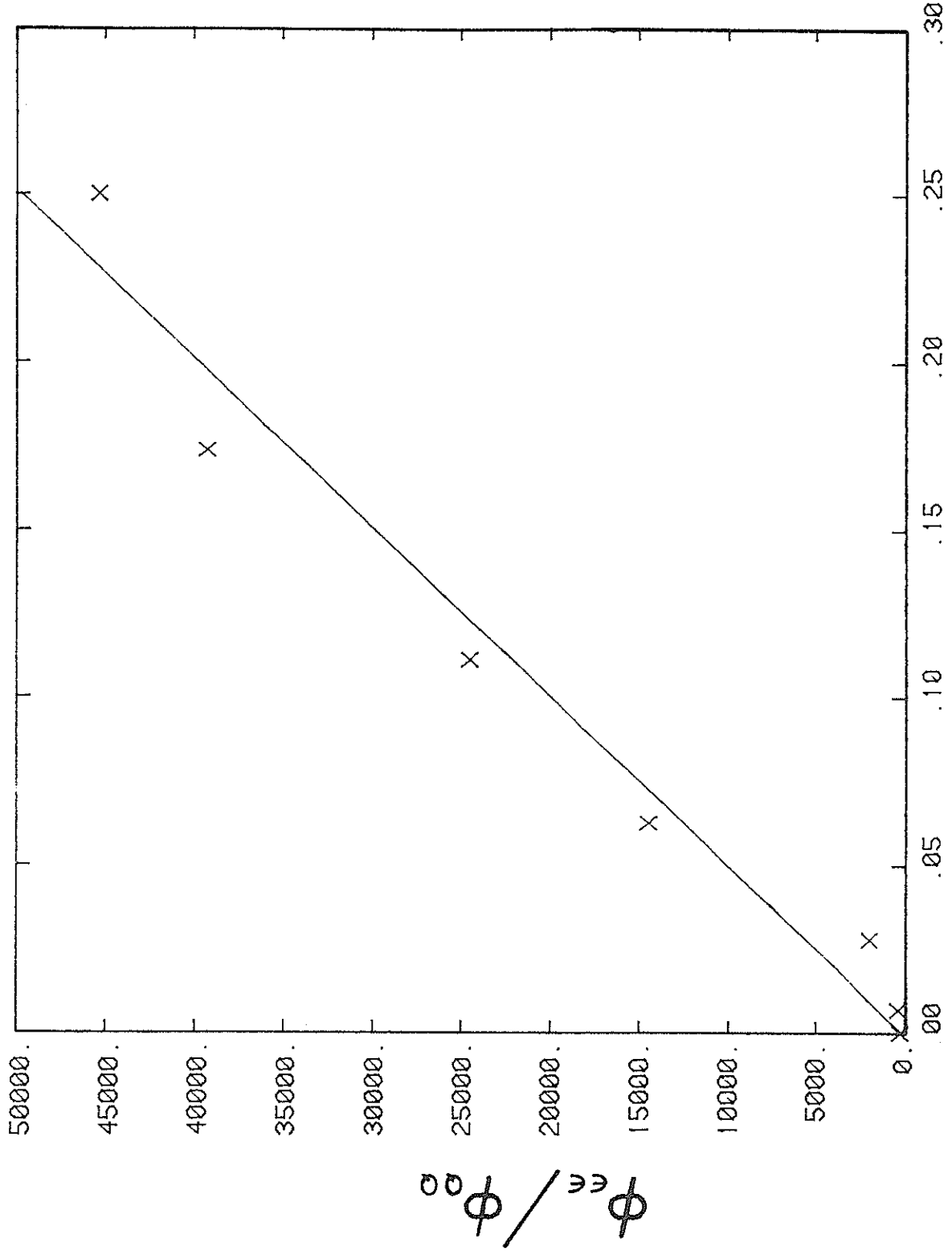

Fig. 19. Regression line for Eq. (28).

or

$$r = 8.82\ \%$$

$$\frac{S_y^2}{a^2 r^2} = 198294.95\ \text{weeks}^2$$

or

$$\frac{S_y^2}{a^2} = 1542.58\ \text{weeks}^2$$

$$\frac{S_y}{a} = 275\ \text{days} \qquad (29)$$

To compute S_y we must first estimate a, the outflow constant. We approximate the Paul Spring aquifer by a converging flow system (Fig. 20). The spring is located at the point of convergence, the single point of outflow. Two lines are drawn from this point of convergence to enclose the aquifer (Fig. 10). Using the angle between these two lines and the area of the aquifer (assumed to be 0.8 x recharge area) a characteristic length, L, is computed (Fig. 20). For a converging flow system the outflow constant, a, is (Flores and Gelhar, 1976)

$$a = 1.07\ T/L^2 \qquad (30)$$

where

T = transmissivity $[L^2/T]$

also

$$T = Kh_o$$

where

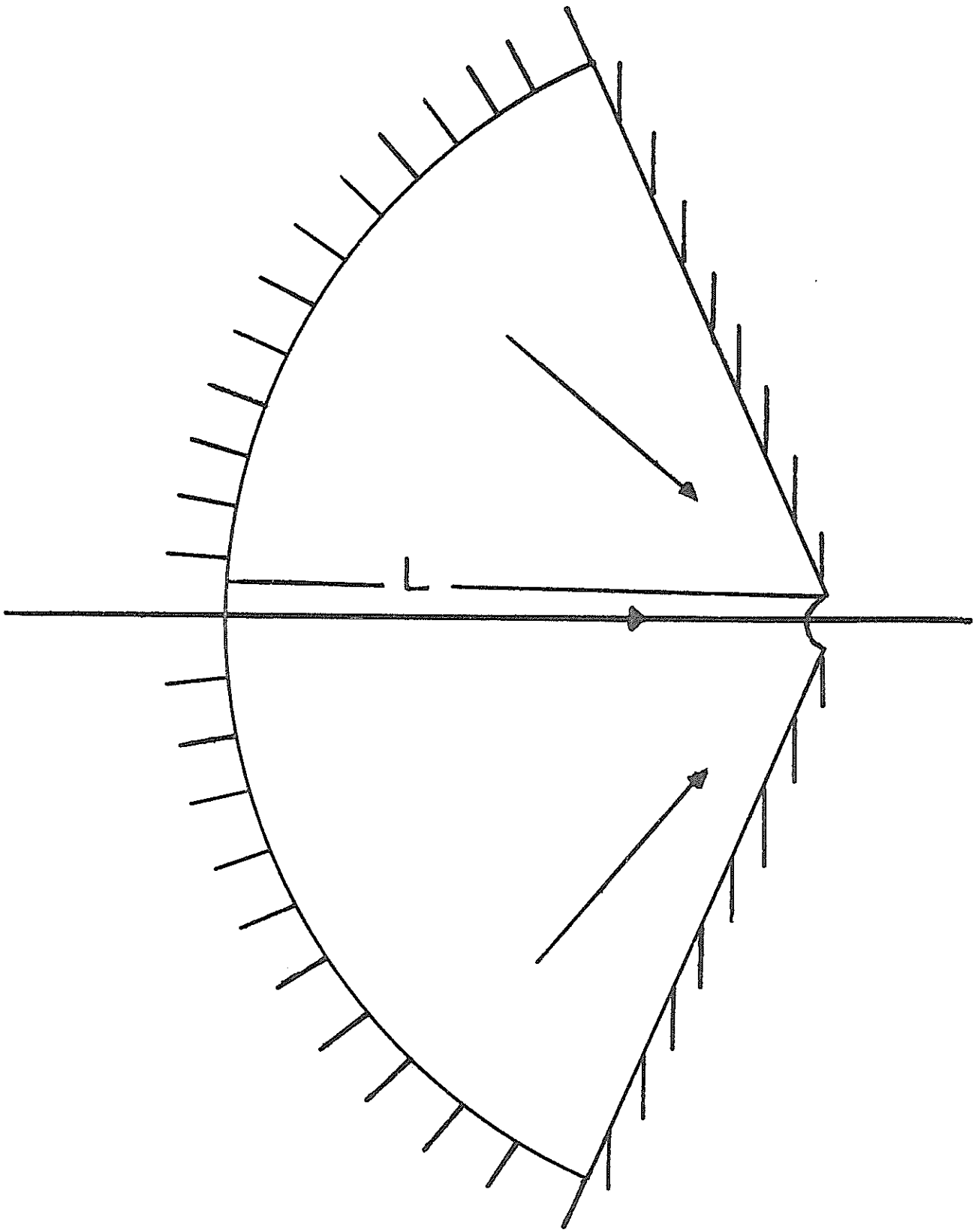

Fig. 20. The two-dimensional converging flow system and its characteristic length (L).

K = hydraulic conductivity [L/T]

h_o = saturated thickness [L] .

Assuming an average value for $\underline{K}$ of 10^{-4}gal/d-ft^2, and an aquifer thickness of 25 ft.

$$T = 33{,}422 \text{ ft}^2/\text{d};$$

also, from Figs. 10 and 20

$$L = 6090 \text{ ft.}$$

Substituting these values of $\underline{T}$ and $\underline{L}$ into Eq. (30)

$$a = 0.000964/\text{day} = 0.00675/\text{week.}$$

and, from Eq. (29)

$$S_y = 6.9\%$$

Numerical Model with a Deep Flow Component

In this model we assume that the springflow is derived from two sources. The first is recharge from precipitation, and the second is water from a deep regional flow system. At present, we are unable to measure the deep flow component (D) directly, so we estimate it in two different ways. The first estimate of D is a constant taken as the lowest recorded spring flow, and the second is a linear function that follows the long-term trend of the springflow (Fig. 14). The constant value of D is 34.8 gpm. The linear function is given by the sloping line in Fig. 14.

$$D = 34.8 + 0.02554(453-N) \text{ gpm}$$

where N = number of days after the first day of record.

We can now write Eq. (11) in terms of a new variable QD, where $QD \equiv Q - D$.

The new equation is

$$\frac{S_y}{a}\frac{d(QD)}{dt} + QD = R = Arp \qquad (31)$$

Eq. (31) is solved by the same methods used to solve Eq. (12). The daily recharge values and graphical results of the solution of Eq. (31) using the Simpson rule and finite difference methods closely resemble the results of Eq. (12) and are not presented here. The final results are shown in Table VIII (p. 87).

As in the case described above, there is no clearly defined maximum in the cross covariance. Table VII (p. 71) gives some recharge percentages calculated for different lag times.

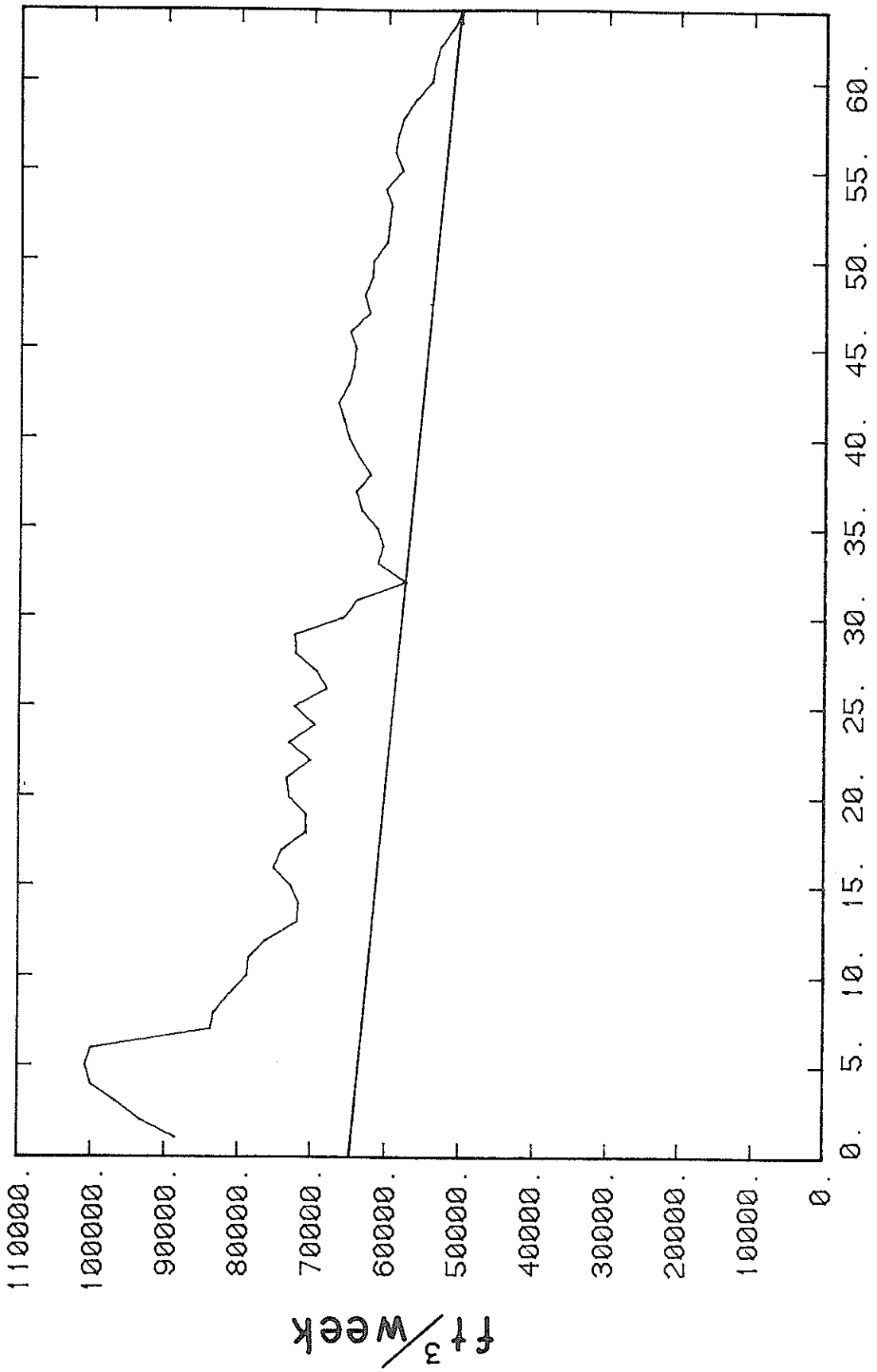

Fig. 21. Weekly springflow and linearly varying deep flow component vs. time.

Stochastic Method with a Deep Flow Component

The case where D is a constant will yield the same results as when D was neglected because the theory of the stochastic method assumes that the data series has a zero mean. The TIMANL computer program subtracts the mean value from every term in the series. Subtracting a constant from each term in the series changes the mean value but does not alter the zero mean series. The linear function D, however, does change the zero mean series. The weekly totaled spring flow and the linear estimates of D are given in Fig. 21. The equation for the line in Fig. 21 is

$$D = 49899.47 + 235.82875(64-M) \text{ ft}^3/\text{week}$$

where

64 = total number of weeks

M = number of weeks from the beginning.

We rewrite Eq. (11) in terms of the new variable QD defined above, and obtain Eq. (31).

The derivation of the solution is identical to that of (22) with Q now replaced by QD. The new spectral equation is

$$\frac{\phi_{\epsilon\epsilon}}{\phi_{QDQD}} = \frac{\omega^2 S_y{}^2}{a^2 r^2} + \frac{1}{r^2} \quad . \tag{32}$$

The regression line for Eq. (32) is presented in Fig. 22. The value of r obtained from the regression is 2.6%. This value is less than those calculated with numerical methods. However, the record

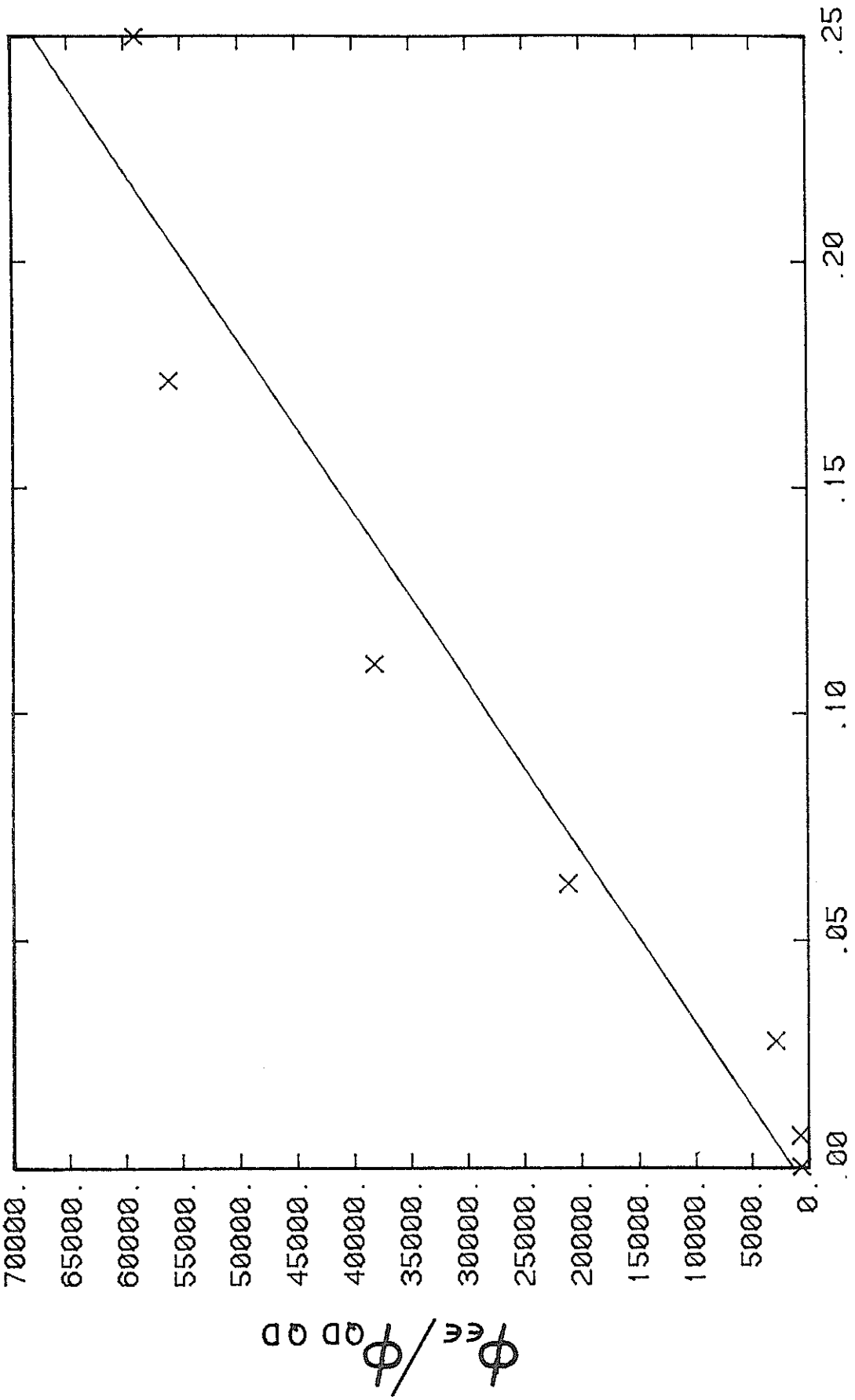

Fig. 22. Regression line for Eq. (32).

is not long enough for a satisfactory application of the stochastic method.

The response time, computed from the regression line slope, is 94 days.

All computational results are summarized in Table VIII.

Table VIII. Summary of Computed Parameters

	Recession curve anal.	Simpson's rule	Finite difference	Cross covariance Rechge/spring	Cross covariance Precip/spring	Spectral analysis
Hypothesis 1: all springflow is derived from precipitation falling on the spring's recharge area						
Response time (d)	48					275
Total net rechge (ft^3)		4.17×10^6	4.18×10^6			
Rechge fraction (%)				28-18*	18.3	8.8
Lag time (d)				0-200*	191	
Hypothesis 2: recharge by precipitation is superposed on a deep flow component of 34.8 gpm						
Response time (d)						275
Total net rechge (ft^3)		1.14×10^6	1.14×10^6			
Rechge fraction (%)				7.6-5.0*		8.8
Lag time (d)				0-200*		
Hypothesis 3: recharge by precipitation is superposed on a deep flow component linearly decreasing from 46.4 gpm to 34.8 gpm						
Response time (d)						94
Total net rechge (ft^3)		7.43×10^5	7.43×10^5			
Rechge fraction (%)				4.9-3.2*		2.6
Lag time (d)				0-200*		

*See Table VII.

Discussion

The calculations have yielded a rather wide range of numbers for the total recharge, the recharge percentage, and the lag time. We now discuss the possible significance of these results in the light of the techniques used to obtain the measurements and of hydrogeologic conditions that might be invoked to justify the results.

The short-term fluctuations of springflow were interpreted as recession curves following individual or closely spaced rainfall events. Unsuccessful attempts were made to correlate these features with temperature, atmospheric pressure, and recharge. A correlation with precipitation was obtained but it is questionable. Thus, the possibility can not be discounted that these features are artifacts. They could be due to unrecognized changes in man-caused withdrawals from the spring or to periodic plugging and spontaneous unplugging of the weir or of the stilling well by debris or bacterial growth, not apparent from the records and undetected in our periodic inspection of the setup.

The long-term decline of the springflow could also be an artifact, caused by progressively developing leakage ahead of or bypassing the weir, for example. This again was not apparent to careful periodic inspections of the system.

Given these uncertainties, which we hope to clear up by further measurements now in progress, we suggest some plausible physical explanations for the computed parameters.

The lag time seems to be quite long for such a small system in highly fractured limestone, even if allowance is made for the uncertainties in the statistical correlation. This may be the effect of the Glorieta Sandstone. The upper tongue of the massive unfractured sandstone lies between the land surface and the water table throughout most of the recharge area. It is thickest in the vicinity of Paul Spring and thins out southwestward away from the spring (Fig. 9). This sandstone is thought to slow down the movement of the recharge waters percolating through the limestone. The sandstone could act like a filter and increase the nonlinearity of the recharge/precipitation relation. A lag time of the order of 100 to 200 days is at least possible.

The recharge percentage corresponding to a lag of 200 days is about 18%, assuming that all of the springflow is derived from local precipitation. The tritium measurements, however, indicate that, on the average, only about 18% of the springflow should be assigned to local precipitation. Thus, the actual recharge percentage would be of the order of $0.18 \times 0.18 \approx 0.03$, or 3%. This is of the same order as computed stochastically with the assumption of a linear underflow contribution to the springflow.

Clearly, further measurements and better control of the experimental parameters are called for. As of now, we have obtained some rough estimates that can help us in planning future research.

COMPARISON OF FACTORS AFFECTING RECHARGE OF THE PAUL SPRING AREA AND THE PRINCIPAL INTAKE AREA

In order to estimate whether or not recharge percentages obtained for the Paul Spring area are applicable to the entire Roswell basin we must examine the physical factors which affect the recharge process. Among these many factors are climate, topography, vegetation and soil type, and/or outcrop type. In discussing these parameters it is necessary to distinguish between the Principal Intake Area, defined by Fiedler and Nye (1933, p.246), who estimated it at 1,200 square miles, and the total recharge area, which they estimated at 4,000 square miles.

The climate of the Paul Spring area has been previously discussed. General comments about the climate are applicable to the entire basin with the exception that a significant amount of snow falls in the higher elevations during the winter months. Table I shows a comparison of precipitation amounts for Elk, which is within 1 mile of Paul Spring, for Roswell, and for the basin average (Gross et al., 1976). Roswell is located near the northeastern edge of the Principal Intake Area (Fig. 2). This table also shows average annual temperatures for Elk and Roswell.

From Table I it can be seen that the Paul Spring region, i.e. Elk, is more humid than either Roswell or the basin in general. It should be mentioned, however, that climatic conditions at Roswell represent the lowest and therefore the driest part of the Principal Intake Area. Table I suggests that in just considering climate

factors alone the recharge percentage for the Paul Spring area could be higher than for the Principal Intake Area.

The topography of an area has a direct effect on the runoff and therefore on the recharge. As mentioned earlier, the Paul Spring area lies on the southeastern edge of the Sacramento Mountains. The slopes in this area are generally steeper than those commonly found in the basin and considerably steeper than the slopes encountered in most of the Principal Intake Area. This suggests that runoff in the study area is greater and that the Paul Spring recharge estimates, adjusted for climate, may be too low for the Principal Intake Area and for the basin in general. Therefore the effect of steeper slopes could possibly cancel out the previously discussed effect of climate.

One of the most important physical factors influencing recharge is probably the type of soil covering the recharge area. The soil types in the recharging areas of the basin (that is, excluding a 15-25 mi. strip adjacent to the Pecos River) fall into three great groups (Anderson et al., 1974). Going from west to east as the elevation decreases and mean annual temperature increases, these are the Haploborolls-Cryoborolls of the western mountainous region, the frigid and mesic Calciustolls-Rockland soils of a north-south strip which includes the Paul Spring area, and the Thermic Calciustolls-Rockland soils of the Principal Intake Area (Anderson et al., 1974). There are significant differences between the soils of the Paul Spring area and those of the mountains to the west. The Haploborolls-Cryoborolls are much thicker, generally about 20 inches thicker, and

contain much more organic material and clayey loam than do the Calciustolls-Rockland soils. This would cause the recharge percentages for Paul Spring to be too high for the western mountainous region of the Roswell artesian basin.

The change from frigid and mesic temperature Calciustolls-Rockland soils to Thermic Temperature Calciustolls-Rockland soils is related to climate and vegetation. The latter soils occur in a dryer area with less vegetation. They are 4 to 20 inches thick, composed of 35-75% angular limestone fragments, and well drained (Anderson et al., 1974). Even though the climate is dryer in the Principal Intake Area, the slopes are flatter and soils more permeable than at Paul Spring. It is therefore assumed that recharge percentages calculated for this study are typical for most of the Roswell artesian basin except the higher Sacramento Mountains and the alluvial strip adjacent to the Pecos River.

The preceding discussion is, admittedly, highly speculative. It is offered as a guide to future research.

RECHARGE FROM THE WESTERN PORTION OF THE ROSWELL BASIN

Fiedler and Nye (1933) assumed that the Yeso Formation was too impervious to allow much water to flow laterally eastward and into the San Andres Formation.

Paul Spring provides a model demonstrating on a small scale the viability of such flow.

A most important feature of this model is the Yeso Formation's anisotropy. Downward percolation through the lower San Andres (Glorieta Sandstone) and upper Yeso formations appears to be restricted. After passing through this semipermeable zone, the water then flows through a relatively unsaturated zone below the semipermeable layer until it intersects another boundary or the regional water table.

On the other hand, the longitudinal conductivity of the silts in the upper Yeso Formation is not negligible; it is aided by solution and collapse features of associated gypsum beds (see section on Geology). In the semipermeable zone, this longitudinally transmitted water then mingles with water recharged directly from the surface, especially where aided by solution and collapse features. The tritium measurements at Paul Spring indicate that this direct contribution is only about a fifth of the total.

At the western boundary of the Principal Intake Area the dip of the Yeso and San Andres formations is small and toward the east. Hence, the most important permeability for movement of water from the Yeso into the San Andres Formation is the longitudinal permeability

(Fig. 23). The lithology of the Yeso Formation over the entire basin is variable but does not change drastically from place to place (Kelley, 1971). The most impermeable beds within the Yeso appear to be siltstones such as those found in the Paul Spring area.

The observation well logs from the interfluvial divides in the Principal Intake Area (Gross et al., 1976) indicate that groundwater is transmitted primarily through the same stratigraphic horizons as at Paul Spring. With Paul Spring, they share relatively low tritium values. If a substantial amount of water were flowing through the upper part of the Yeso Formation into the San Andres Formation, mixing of these "old" waters with "young" locally originated recharge waters could yield low tritium concentrations, consistent with the picture here outlined and with the tritium concentrations actually recorded.

The previous considerations suggest that flow variations at Paul Spring may be correlatable with water level changes in the interfluvial observation wells. Much longer springflow records than we have available would be required for this purpose.

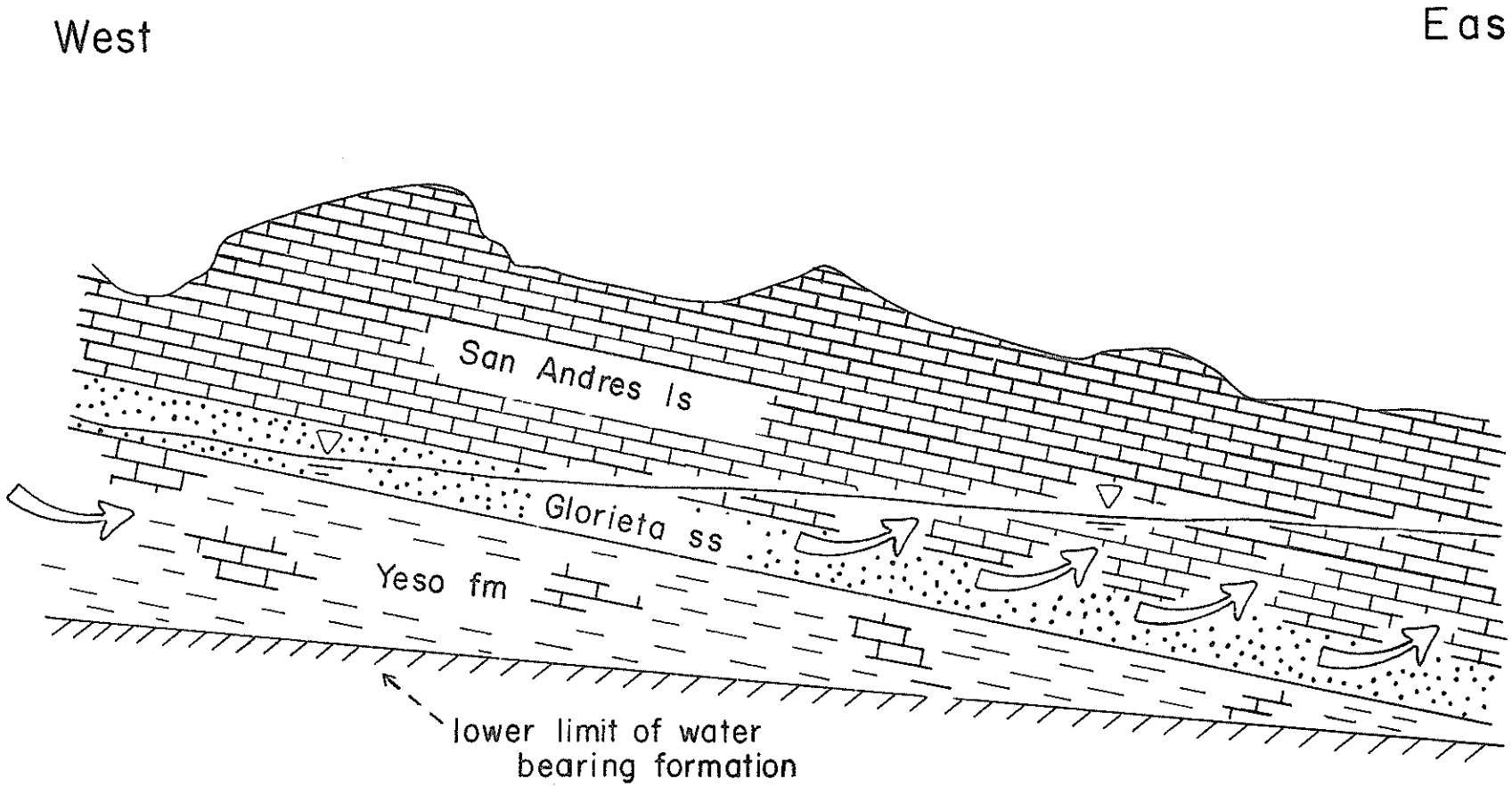

Fig. 23. Idealized model of deep recharge to the San Andres Formation.

SUMMARY OF CONCLUSIONS

Paul Spring issues from a perched body of ground water which is held above other water tables in this area by the upper portion of the Yeso Formation.

The recharge area for Paul Spring is approximately 14,160,440 square feet.

The Glorieta Sandstone acts as a filter, dampening the effect of individual precipitation events on the springflow record.

Dissolution and redeposition of lime and gypsum is presently occurring in the Paul Spring ground water system.

Channeling of water through collapse features and solution breccias is the main factor controlling lateral movement of ground water in the Paul Spring aquifer.

The lag time between precipitation input and springflow output could not be estimated with certainty. It seems to lie between 90 and 200 days.

The average percentage of precipitation which becomes recharge to the Paul Spring aquifer is 3%.

Stochastic representation of the recharge process of the Paul Spring aquifer requires a longer series of springflow measurements than was available. Besides yielding values of the recharge percentage, this method could also give an estimate of an average specific yield of the aquifer.

Tritium analyses indicate that there are two components of flow contributing to waters issuing from Paul Spring. One component is

the flow of relatively "older" water from the upper Yeso Formation (about 80%) and the remainder is relatively "younger" water of the lower San Andres Formation.

Eastward ground water flow through the upper Yeso Formation is the cause of low tritium values in the Principal Intake Area.

Recharge in the western Roswell artesian basin contributes a significant amount of water to the Principal Aquifer of the Roswell artesian basin.

The conclusions reached in this work are only tentative. To affirm them it is necessary to have a longer series of springflow measurements. Springflow measurements at Paul Spring should then be compared to water level changes in observation wells of the Principal Intake Area.

LIST OF REFERENCES

Anderson, J. U., V. G. Link, H. E. Dregne, and H. J. Maker (1974): Soils of New Mexico. Research Report 285. New Mexico State University. Agricultural Experiment Station. Las Cruces, NM.

Bean, R. T. (1949): Geology of the Roswell Artesian Basin, New Mexico, and Its Relation to the Hondo Reservoir. Technical Report No. 9. State of New Mexico, State Engineer Office. Santa Fe, NM, 1951. (36 pp.).

Dooge, J. C. I. (1960): The Routing of Linear Recharge Through Typical Elements of Linear Storage. Publication 52, pp. 286-300. International Association of Scientific Hydrology (IASH), Helsinki.

Duffy, C. J., L. W. Gelhar, and G. W. Gross (1978): Recharge and Groundwater Conditions in the Western Region of the Roswell Basin. Report No. 100. New Mexico Water Resources Research Institute. New Mexico State University Las Cruces, NM (111 pp.).

Eriksson, E. (1970): Groundwater Time Series: An Exercise in Stochastic Hydrology. J. Nord. Hydrol. 1 (3), 181-205.

Fiedler, A. G., and S. S. Nye (1933): Geology and Ground-Water Resources of the Roswell Artesian Basin, New Mexico. U.S.G.S. Water Supply Paper 639. (372 pp.).

Flores, W., A. E. Z., and L. W. Gelhar (1976): A Stochastic Management Model for the Operation of a Stream-Aquifer System. Report No. 075. New Mexico Water Resources Research Institute. New Mexico State University, Las Cruces, NM. (209 pp.).

Gelhar, L. W. (1974): Stochastic Analysis of Phreatic Aquifers. Water Resour. Res. 10 (3), 539-545.

Gelhar, L. W., and J. L. Wilson (1974): Ground Water Quality Modeling. Groundwater 12 (6), 399-408.

Gross, G. W., R. N. Hoy, and C. J. Duffy (1976): Application of Environmental Tritium in the Measurement of Recharge and Aquifer Parameters in a Semi-Arid Limestone Terrain. Report No. 080. New Mexico Water Resources Research Institute. New Mexico State University. Las Cruces, NM (212 pp.).

Gross, G. W., and R. N. Hoy (1979): Recharge in Semiarid Mountain Environments. Technical Completion Report (Project A-055-NMEX). New Mexico Water Resources Research Institute. New Mexico State University. Las Cruces, NM. (In preparation).

Hantush, M. S. (1957): Preliminary Quantitative Study of the Roswell Ground-Water Reservoir, New Mexico. New Mexico Institute of Mining and Technology Research and Development Division. Socorro, NM (118 pp.).

Havenor, K. C. (1968): Structure, Stratigraphy, and Hydrogeology of the Northern Roswell Artesian Basin, Chaves County, New Mexico. Circular 93. State Bureau of Mines and Mineral Resources. New Mexico Institute of Mining and Technology. Socorro, NM (30 pp.).

Jacob, C. E. (1944): Correlation of Ground-Water Levels and Precipitation on Long Island, New York. Trans. A. G. U. 25, 564-573.

Kelley, V. C. (1971): Geology of the Pecos Country, Southeastern New Mexico. Memoir 24. State Bureau of Mines and Mineral Resources. New Mexico Institute of Mining and Technology. Socorro, NM (75 pp.).

Kinney, E. E., J. D. Nations, B. J. Oliver, P. G. Wagner, T. A. Siwula, and R. E. Renner (1968): The Roswell Artesian Basin. The Roswell Geological Society. Roswell, NM (32 pp.).

Leupold and Stevens, Inc. (1975): Stevens Water Resources Data Book. Leupold and Stevens, Inc., Beaverton, Oregon.

Lumley, J. L., and H. A. Panofsky (1964): The Structure of Atmospheric Turbulence. Wiley, New York, NY (239 pp.).

Mourant, W. A. (1963): Water Resources and Geology of the Rio Hondo Drainage Basin. Technical Report 28. New Mexico State Engineer. Santa Fe, NM (85 pp.).

Nir, A. (1964): On the Interpretation of Tritium Age Measurements of Groundwater. Jour. Geophys. Res. 69, 2589-2595.

Rabinowitz, D. D., and G. W. Gross (1972): Environmental Tritium as a Hydrometeorologic Tool in the Roswell Basin, New Mexico. Report No. 016. New Mexico Water Resources Research Institute. New Mexico State University. Las Cruces, NM (268 pp.).

Rabinowitz, D. D., G. W. Gross, and C. R. Holmes (1977): Environmental Tritium as a hydrometeorologic tool in the Roswell Basin, N.M. Jour. Hydrol. 32, 3-46.

Renick, B. C. (1926): Geology and Ground-Water Resources of the Drainage Basin of the Rio Penasco above Hope, New Mexico. 7th. Biennial Report, pp. 103-138. New Mexico State Engineer. Santa Fe, NM.

Updegraff, C. D., and L. W. Gelhar (1978): Parameter Estimation for a Lumped-Parameter Ground-Water Model of the Mesilla Valley, New Mexico. Report No. 097. New Mexico Water Resources Research Institute. New Mexico State University. Las Cruces, NM (69 pp.).

Wastler, T. A. (1969): Spectral Analysis; Application in Water Pollution Control. CWT-3. Federal Water Pollution Control Administration. U. S. Dept. Int.

APPENDIX A

LOCAL WELL LOG DATA FOR THE PAUL SPRING AREA
(from open files at the New Mexico State
Engineer office, Santa Fe, New Mexico)

Location: 16.16.5.434

Approximate water table elevation: 5680'

Depth to water: 130'

Depth (ft)		Thickness (ft)	Color	Description
From	To			
0	2	2	black	top soil
2	10	8	white	caliche and gravel
10	60	50	gray	rock and gravel
60	75	15	gray	lime
75	80	5	gray	gravel
80	110	30	gray	lime
110	140	30	yellow	clay
140	165	25	red	clay
165	190	25	gray	rack and gravel
190	227	37	gray	lime
227	235	7	brown	sand, lime; water
235	245	10	gray	lime
245	265	20	red	clay
265	275	10	gray	gravel
275	287	12	red	clay

Location: 16.16.10.24131

Approximate water table elevation: 5706'

Depth to water: 14'

Depth (ft)		Thickness (ft)	Color	Description
From	To			
0	5	5		dirt
5	14	9		lime
16	85	69		gravel and boulders; water
85	120	35		lime
120	140	20	yellow	sand; water

Location: 16.16.11.41111

Approximate water table elevation: 5658'

Depth to water: 12'

Depth (ft)		Thickness (ft)	Color	Description
From	To			
0	15	15	gray	rock; water
15	85	70	black	rock
85	97	12		gravel; water
97	130	33	gray	rock
130	190	60	yellow	clay
190	225	35	black	rock
225	230	5		no sample; water
230	235	5	blue	clay

Location: 16.16.12.31143

Approximate water table elevation: 5666'

Depth to water: 9'

Depth (ft)		Thickness (ft)	Color	Description
From	To			
0	45	45	gray	rock
45	50	5	yellow	sand, water
50	358	308	gray	rock
358	374	16		crevice-no sample; water

Location: 16.16.12.320

Approximate water table elevation: 5640'

Depth to water: 20'

Depth (ft)		Thickness (ft)	Color	Description
From	To			
0	30	30		rock
30	35	5		gravel-water
35	42	7		rock

Location: 16.16.17.33322

Approximate water table elevation: 5718'

Depth to water: 182'

Depth		Thickness (ft)	Color	Description
From	To			
182	192	10	gray	lime
192	207	15	brown	lime
207	217	10		sandy lime; water
217	225	8	gray	lime

Location: 16.16.30.441422

Approximate water table elevation: 5240'

Depth to water: 260'

Depth (ft)		Thickness (ft)	Color	Description
From	To			
0	15	15		top soil
15	260	245		hard lime
260	270	10		sand; water
270	275	5		lime
275	280	5	red	clay

Location: 16.16.8.314

Approximate water table elevation: 5768'

Depth to water: 92'

Depth (ft)		Thickness (ft)	Color	Description
From	To			
0	42	42		gravel and dirt
42	112	70		limestone
112	117	5		rock with crevices; water
117	190	73		limestone
190	200	10		coarse gravel; water
200	204	4		limestone

APPENDIX B

SPRINGFLOW MEASUREMENT PROCEDURE, EQUIPMENT AND PROBLEMS

The flow from Paul Spring was monitored with the aid of a Stevens Type-F water level recorder. A stilling pond was constructed approximately 25 feet downstream of the spring's point of issuance. All equipment used is shown in Figure 24. This pond was lined with plastic to prevent leakage. The pond's dam consisted of a 2 foot by 4 foot sheet of plywood with an aluminum 90° V-notch weir mounted on it. In order to increase the sensitivity of measurement, the notch angle was changed to 22½° after 1½ months. The Type-F recorder was then placed on top of a stilling well installed in the pond. The Type-F recorder was equipped with a 30-day battery-powered clock drive unit. The recorder chart was changed every 30 days and the water level was measured by hand to insure continued accuracy. The formula used to calculate the quantity of flow thru a 22½° weir is (Leupold & Stevens, Inc., 1975):

$$\text{gallons per minute} = 225.05 \times H^{5/2}$$

where

H = height of the water in the V-notch.

It is important to discuss the difficulties with flow measurement encountered in this study. The springflow is assumed to be the total flow from this perched system. Therefore, the accuracy of the recharge percentages obtained is directly related to the accuracy of the flow measurement.

The first difficulty in measuring the flow of Paul Spring was the existence of a pipe at the mouth of the spring. Water flowing

SPRINGFLOW RECORDING EQUIPMENT

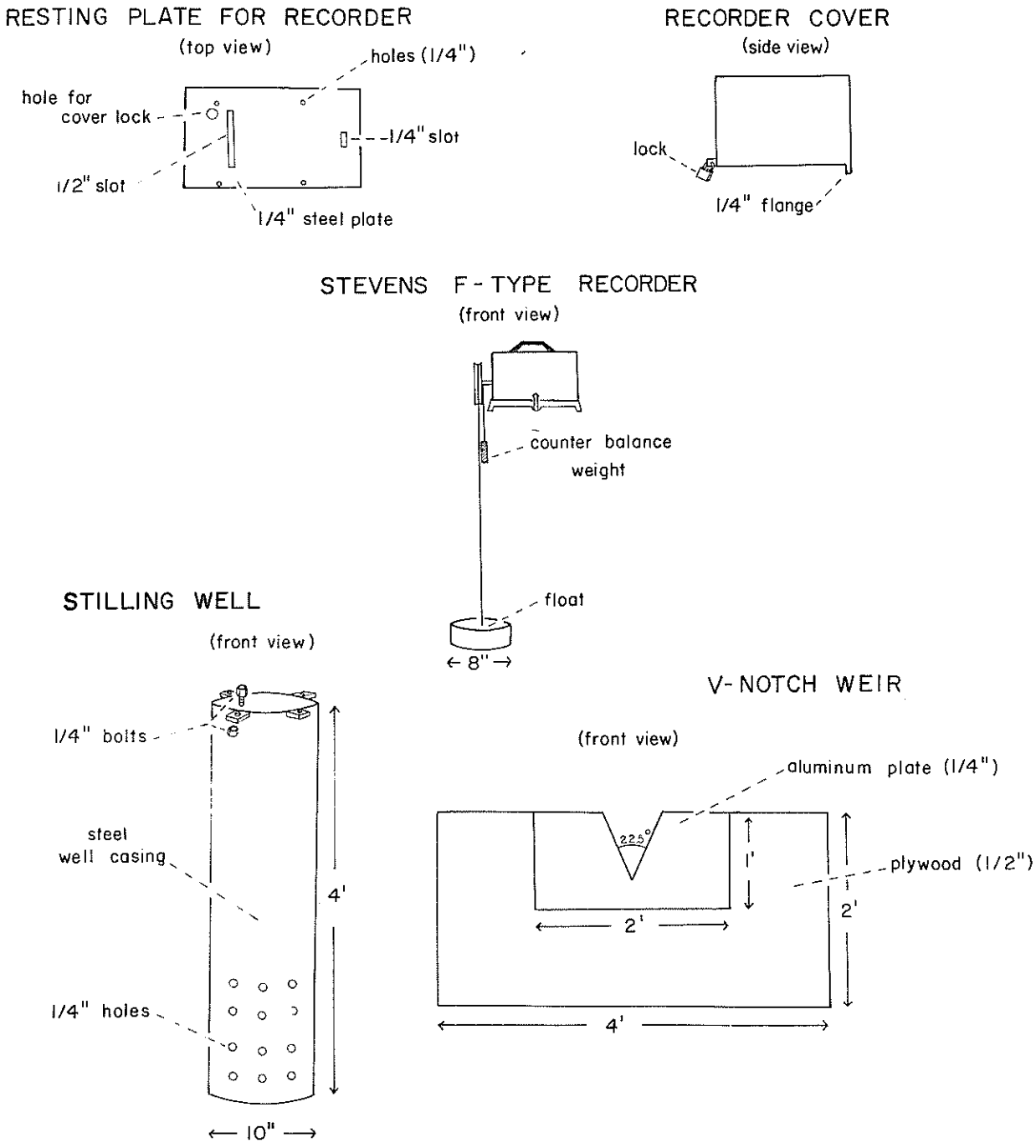

Fig. 24. Schematic of the weir and stilling well.

continually through this pipe provides water for domestic use at the Charles Mulcock residence. The pipe is 1 inch in diameter and, according to Mr. Mulcock, calcium carbonate has considerably clogged the pipe. The flow from this pipe was measured several times during the course of this study. The amount of water flowing through this pipe was found to be a nearly constant value of one percent of the total flow. This quantity was added into the total flow calculations.

Other flow not measured by the Stevens recorder includes what appeared to be leakage through the walls of the pond. Since the pond was lined with plastic it is doubtful that this water was actually derived from the pond. It is more likely that this water represented direct flow from the perched system. The amount of water escaping in this manner was not large. It was estimated to be a nearly constant quantity of 2% of the springflow. This amount was also taken into account in total flow calculations.

There were several factors which adversely affected the records obtained using the Type-F recorder. The most serious of these resulted from debris clogging the 22½° V-notch. This problem was overcome by covering part of the stilling pond, including the V-notch, with chicken wire. Another error in flow records was a result of the stilling well design. Since there were several rows of holes in the stilling well, some water flowed through the well. This water brought in debris which clogged the stilling well holes. To remedy this problem all but one row of holes in the stilling well were plugged. A small mesh wire was also placed around the stilling well about 2

inches from it. Clogging was also caused by the formation of a thin film over the stilling well holes, probably bacterial in nature. This problem was more difficult to overcome because any chemical placed in the stilling well to retard bacterial growth would soon be washed away.

The problems mentioned above caused discrepancies between the measurements recorded on the Type-F chart and the field measurements made at the time the charts were changed, that is at the end of each 30-day period. These differences were evident on several of the recorder charts. The procedure used to correct for these errors in flow measurement was as follows. First, the charts were inspected for abrupt changes or jumps in the flow record. The fluctuations were assumed to have been caused by the actual clogging of either the holes in the stilling well or of the V-notch weir. A new record was then constructed by neglecting these jumps and realigning the flow record across them. An example is shown in Fig. 25.

For most of the records this method produced values which matched the field measurements made at the time the charts were changed. When these values did not match, linear interpolation was used to adjust the chart values to match the field measurements. It should be noted that for the charts subjected to linear interpolation, the largest difference to be adjusted for was about .02 inches.

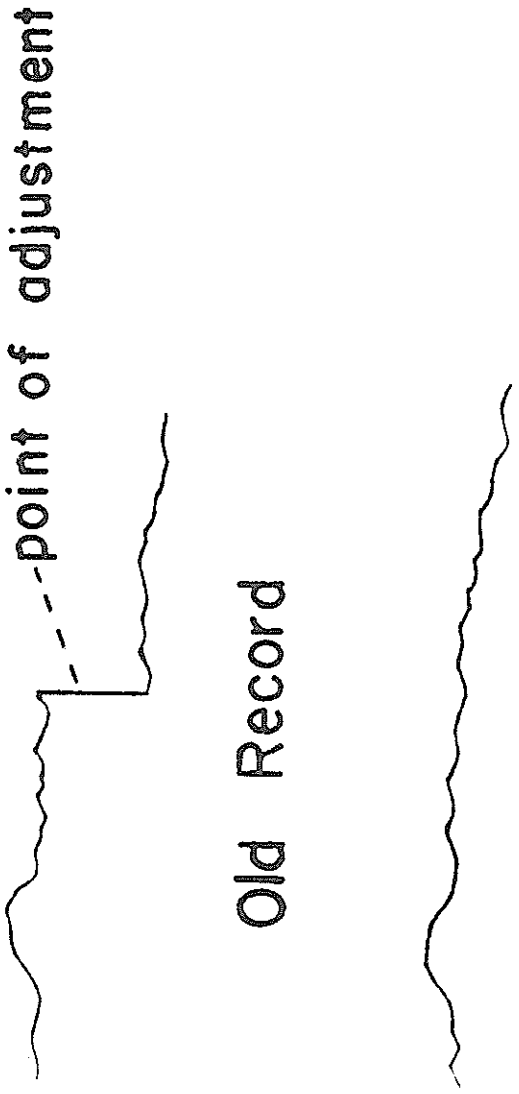

Fig. 25. Adjustment of flow record.

APPENDIX C

DAILY AVERAGE SPRINGFLOW

DAILY AVERAGE SPRINGFLOW 1977, gpm

DAY	JAN	FEB	MAR	APR	MAY	JUN	JUL	AUG	SEP	OCT.	NOV	DEC
01		75.1	61.1	52.3	54.9	53.5	50.7	50.2	45.6	47.6	48.2	46.8
02		75.0	60.8	52.1	52.6	51.7	49.7	51.3	45.2	47.7	48.0	47.2
03		74.9	59.9	52.4	52.3	51.7	51.0	49.0	45.6	47.2	47.9	47.2
04	63.9	74.6	60.3	52.8	51.9	50.6	49.2	47.9	45.8	47.6	47.8	47.4
05	64.7	74.8	60.0	53.2	51.6	52.2	48.1	47.3	46.1	48.1	47.8	47.1
06	65.6	75.0	60.1	53.3	52.2	51.8	50.3	45.8	46.8	47.9	47.4	46.7
07	66.0	74.0	59.1	53.0	53.1	53.6	53.1	45.8	46.6	48.1	48.0	46.7
08	66.1	74.3	58.3	53.0	53.9	53.1	52.5	44.9	46.6	48.3	48.2	46.9
09	66.4	74.9	57.1	53.1	53.4	53.1	52.6	43.8	47.0	49.1	48.1	45.7
10	66.8	74.8	56.6	53.5	52.2	54.6	52.8	44.4	47.4	49.7	48.0	45.6
11	67.6	73.8	57.5	54.2	52.5	55.2	51.6	44.9	47.6	49.8	47.6	45.6
12	67.8	74.0	58.1	52.6	52.3	55.5	52.4	40.8	47.9	48.6	47.3	45.6
13	68.6	73.6	60.3	53.5	52.4	56.2	52.8	40.7	48.1	48.5	47.1	45.5
14	69.2	73.4	61.3	54.8	52.7	54.1	53.9	41.3	48.6	48.7	47.6	45.8
15	69.9	68.1	60.7	54.3	52.7	52.3	55.3	42.5	48.3	48.8	48.2	45.9
16	70.4	62.2	60.2	54.7	53.1	50.0	53.0	46.5	48.2	49.4	49.1	45.7
17	70.7	61.7	59.5	55.5	55.3	48.4	53.8	46.9	47.9	49.6	49.0	50.0
18	71.0	62.0	57.1	53.5	55.2	50.9	54.3	45.1	47.6	49.1	48.9	44.5
19	71.0	61.2	57.5	52.8	56.0	52.6	54.7	45.2	45.9	48.9	48.6	43.7
20	71.0	59.4	56.5	54.3	54.9	54.2	56.1	45.0	45.8	48.9	47.7	43.7
21	71.4	59.6	56.5	55.3	54.7	54.2	56.2	44.5	45.9	49.9	47.2	44.1
22	72.1	60.5	56.7	56.7	52.7	55.2	55.7	44.8	46.1	51.2	46.6	44.5
23	72.4	62.1	56.8	56.9	52.5	55.1	53.3	44.5	46.2	49.7	46.2	44.5
24	72.7	63.1	56.7	57.5	53.0	54.8	51.1	44.2	46.4	48.9	45.9	44.8
25	73.5	63.6	56.7	57.7	54.8	53.0	49.7	44.8	46.7	48.3	46.6	44.7
26	73.8	62.3	56.3	56.8	55.8	52.7	49.2	45.0	46.3	48.6	46.4	44.8
27	74.0	60.9	56.2	55.9	56.1	52.4	49.7	45.1	46.8	48.6	46.5	44.8
28	74.3	59.9	56.1	55.1	56.4	51.4	48.6	45.3	47.2	48.6	46.5	44.8
29	74.5		55.3	54.5	53.4	50.7	48.3	45.6	47.9	48.3	46.3	44.7
30	75.1		54.8	55.2	52.9	51.3	46.7	45.6	48.1	48.3	46.6	44.5
31	75.1		54.0		53.8		49.4	45.3		48.3		44.3

DAILY AVERAGE SPRINGFLOW 1978, gpm

DAY	JAN	FEB	MAR	APR
01	44.0	43.8	39.9	34.8
02	43.8	43.6	40.0	
03	43.9	43.0	39.7	
04	43.8	43.2	39.4	
05	43.4	43.5	39.7	
06	44.1	43.3	39.7	
07	44.0	43.3	39.7	
08	44.5	43.1	39.8	
09	44.6	43.2	39.3	
10	44.8	43.3	39.5	
11	45.1	42.9	39.0	
12	44.7	42.6	39.8	
13	44.8	42.0	39.6	
14	45.2	42.0	39.4	
15	44.9	42.0	38.1	
16	43.8	42.2	37.7	
17	43.3	41.9	37.3	
18	42.8	41.6	37.4	
19	42.9	41.3	38.1	
20	43.3	40.9	38.2	
21	43.2	41.0	38.1	
22	42.8	40.6	37.7	
23	43.1	40.2	37.3	
24	43.6	40.1	37.3	
25	43.4	39.5	36.6	
26	43.4	39.6	36.4	
27	43.9	39.6	35.8	
28	43.8	40.2	35.4	
29	43.9		34.9	
30	44.1		34.8	
31	43.8		34.8	

APPENDIX D

DATES OF THE SPRING FLOW RECESSIONS

AND

THE COMPUTER PROGRAM USED

TO CALCULATE S_y/a

SPRING FLOW RECESSIONS
(See Figure 26)

	DATES	LENGTH IN DAYS
1977	Feb 10 - Feb 20	10
	Feb 25 - Feb 28	3
	Mar 2 - Mar 3	1
	Mar 6 - Mar 10	4
	Mar 14 - Mar 21	6
	Mar 28 - Apr 1	4
	Apr 11 - Apr 12	1
	Apr 17 - Apr 19	2
	Apr 25 - Apr 29	4
	Apr 30 - May 4	4
	May 9 - May 10	1
	May 19 - May 22	3
	May 28 - May 30	2
	Jun 1 - Jun 4	3
	Jun 5 - Jun 6	1
	Jun 13 - Jun 17	4
	Jun 23 - Jun 29	6
	Jun 30 - Jul 2	2
	Jul 3 - Jul 5	2
	Jul 7 - Jul 8	1
	Jul 10 - Jul 11	1
	Jul 21 - Jul 26	5
	Jul 27 - Jul 30	3
	Aug 3 - Aug 9	6
	Aug 17 - Aug 18	1
	Aug 20 - Aug 21	1
	Sep 1 - Sep 2	1
	Sep 17 - Sep 19	2
	Sep 25 - Sep 26	1
	Sep 30 - Oct 1	1
	Oct 2 - Oct 3	1
	Oct 5 - Oct 6	1
	Oct 11 - Oct 12	1
	Oct 22 - Oct 25	3
	Nov 19 - Nov 20	1
	Dec 8 - Dec 9	1
	Dec 18 - Dec 19	1
1978	Jan 4 - Jan 5	1
	Jan 11 - Jan 12	1
	Jan 15 - Jan 18	3
	Jan 21 - Jan 22	1
	Feb 2 - Feb 3	1
	Feb 10 - Feb 13	3
	Feb 24 - Feb 25	1
	Mar 8 - Mar 9	1
	Mar 10 - Mar 11	1
	Mar 14 - Mar 17	3
	Mar 24 - Mar 25	1
	Mar 26 - Mar 29	3

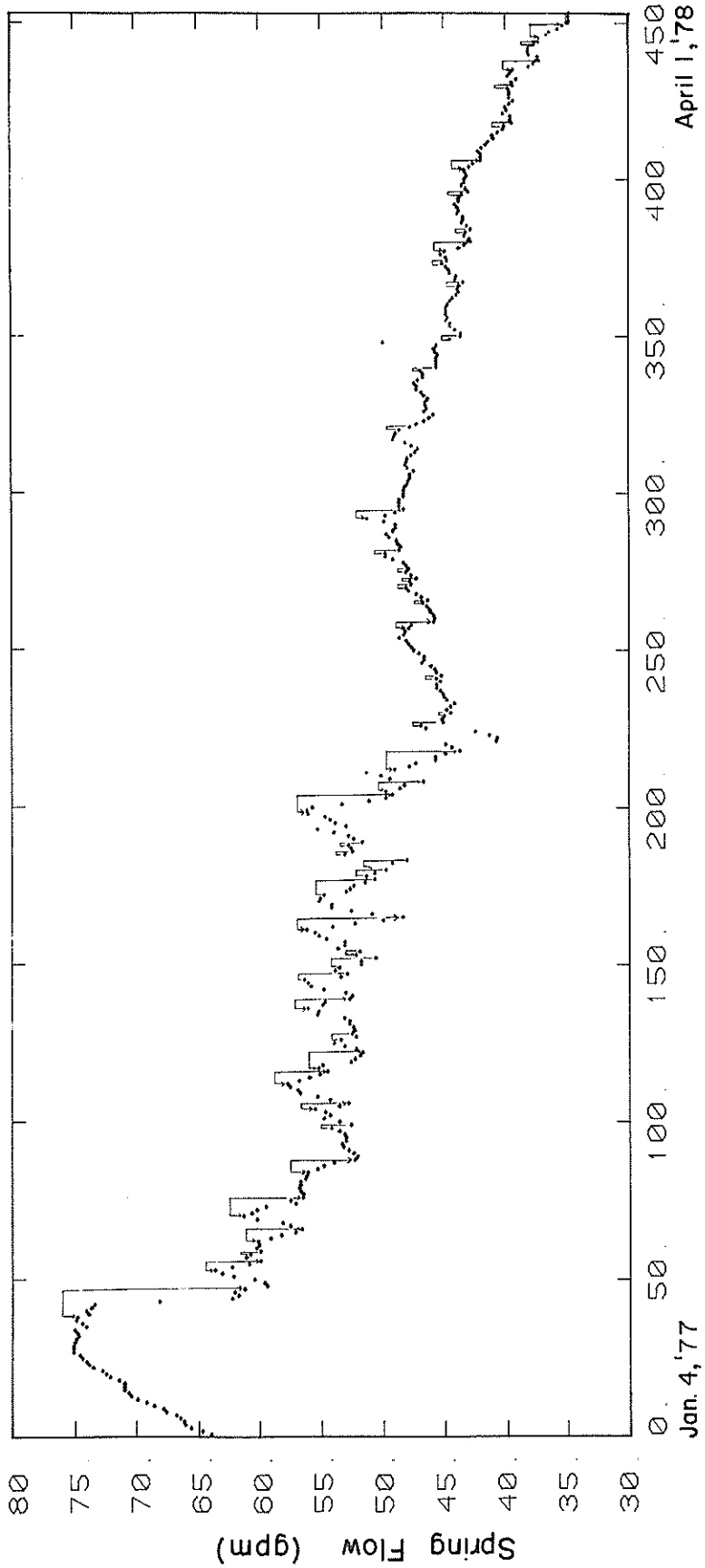

Fig. 20. Spring flow recession events used for analysis.

```
C  PROGRAM TO CALCULATE THE AVERAGE VALUE OF THE
C  HYDRAULIC RESPONSE TIME SY/A.
C
      OPEN (UNIT=1,ACCESS='SEQIN',FILE='RECESS.DA')
      K=-1
      NUNIT=5
      WRITE (NUNIT,150)
 10   READ (1,100,END=12) Q
      K=K+1
      J=J+1
      IF (K.GT.1.AND.Q.EQ.1.00000) K=0
      IF (Q.EQ.1.00000) GO TO 10
      AS=ALOG(Q)/-FLOAT(K)
      SA=1./AS
      SASUM=SASUM+SA
      WRITE (NUNIT,200) K,AS,SA
      GO TO 10
100   FORMAT (F8.5)
150   FORMAT (20X,'A',15X,'S',/,T3,'DELTA T',10X,'---',13X,
     1'---',/,T21,'S',15X,'A')
200   FORMAT (4X,I2,9X,E12.6,6X,F12.6)
300   FORMAT (//,' THE AVERAGE VALUE OF S/A IS  ',F12.6)
 12   AVESA=SASUM/J
      WRITE (NUNIT,300) AVESA
      WRITE (5,300) AVESA
      STOP
      END
```

DELTA T	A/S	S/A
1	.134602E-01	74.293194
2	.537883E-02	185.914050
3	.539001E-02	185.528410
4	.472436E-02	211.668900
5	.187677E-01	53.283168
6	.307440E-01	32.526699
7	.275042E-01	36.358067
8	.234600E-01	42.625771
9	.222970E-01	44.849102
10	.230521E-01	43.380053
1	.206518E-01	48.421964
2	.216887E-01	46.107018
3	.199804E-01	50.049129
1	.149106E-01	67.066338
1	.167800E-01	59.594755
2	.152038E-01	65.772895
3	.170697E-01	58.583352
4	.150012E-01	66.661323
1	.984834E-02	101.539970
2	.905144E-02	110.479700
3	.993321E-02	100.672400
4	.177451E-01	56.353456
5	.127989E-01	78.131507
6	.135892E-01	73.587589
1	.143627E-01	69.625023
2	.117213E-01	85.314601
3	.127162E-01	78.640068
4	.175359E-01	57.025925
1	.299645E-01	33.372844
1	.367055E-01	27.243888
2	.249366E-01	40.101660
1	.157230E-01	63.601240
2	.158485E-01	63.097283
3	.153689E-01	65.066367
4	.142643E-01	70.105037
1	.544479E-02	183.661680
2	.241227E-01	41.454804
3	.179902E-01	55.585865
4	.154103E-01	64.891464
1	.227263E-01	44.001894
1	.198354E-01	50.414847
2	.117418E-01	85.165853
3	.202459E-01	49.392671

1	.546568E-01	18.295972
2	.320346E-01	31.216200
1	.342188E-01	29.223667
2	.171094E-01	58.447333
3	.185782E-01	53.826409
1	.768949E-02	130.047640
1	.380862E-01	26.256256
2	.359575E-01	27.810612
3	.389645E-01	25.664402
4	.373542E-01	26.770734
1	.545485E-02	183.323180
2	.194276E-01	51.473185
3	.148457E-01	67.359392
4	.125603E-01	79.615902
5	.139022E-01	71.931206
6	.138698E-01	72.099281
1	.117690E-01	84.969128
2	.158434E-01	63.117835
1	.359277E-01	27.833643
2	.292703E-01	34.164355
1	.113643E-01	87.994646
1	.229923E-01	43.492804
1	.893984E-02	111.858780
2	.264895E-01	37.750859
3	.317117E-01	31.534070
4	.307284E-01	32.543166
5	.265829E-01	37.618186
1	.223785E-01	44.685668
2	.142872E-01	69.992760
3	.207528E-01	48.186226
1	.227058E-01	44.041537
2	.176530E-01	56.647618
3	.225135E-01	44.417887
4	.168851E-01	59.223850
5	.174757E-01	57.222173
6	.186973E-01	53.483687
1	.391359E-01	25.551977
1	.111722E-01	89.508066
1	.880868E-02	113.524400
1	.627968E-02	159.243880
2	.213233E-01	46.897086
1	.860693E-02	116.185390
1	.104545E-01	95.653000
1	.105353E-01	94.918955

1	.416868E-02	239.884160
1	.243952E-01	40.991745
1	.297378E-01	33.627218
2	.229801E-01	43.515940
3	.194358E-01	51.451527
1	.186936E-01	53.494129
1	.259231E-01	38.575600
1	.181436E-01	55.115835
1	.917194E-02	109.028250
1	.890957E-02	112.238850
1	.248051E-01	40.314264
2	.181401E-01	55.126422
3	.159664E-01	62.631709
1	.930314E-02	107.490600
1	.138555E-01	72.173262
1	.928296E-02	107.724320
2	.815108E-02	122.683100
3	.101599E-01	98.425762
1	.150730E-01	66.343671
1	.126395E-01	79.116765
1	.127408E-01	78.487900
1	.335464E-01	29.809419
2	.220543E-01	45.342590
3	.182577E-01	54.771485
1	.189484E-01	52.774921
1	.166173E-01	60.178230
2	.139272E-01	71.802056
3	.140277E-01	71.287338

THE AVERAGE VALUE OF S/A IS 48.422208

APPENDIX E

COMPUTER PROGRAMS USED TO CALCULATE THE DAILY NET RECHARGE, AND NUMERICAL RESULTS

```
C       ESTIMATION OF RECHARGE USING THE METHOD GIVEN BY UPDEGRAFF
C       AND GELHAR (1977).
c
c       bb=         dummy variable in tridiagonal array solution
c       d=          solution of d-e with recharge = 0
c       Date=       month and day
c       gg=         dummy variable in tridiagonal array solution
c       lamda=      hydraulic rate constant
c       n=          # of observations
c       precip=     amount of each precip event in inches
c       prept=      input of daily precip in inches
c       Q=          spring flow in gallons per minute
c       qin=        estimated initial flow
c       qout=       estimated final flow
c       u=          recharge in Cu-Ft per day
c       z=          spring flow in Cu-Ft per day
c
c
        real q,lamda
        DIMENSION DATE(2,500),D(500),Q(500),GG(500),s(500)
        DIMENSION U(500),BB(500),z(500)
        data nunit/3/
        OPEN (UNIT=31,ACCESS='SEQIN',FILE='SPRING.DAT')
        OPEN (UNIT=32,ACCESS='SEQOUT',FILE='RECHG.DAT')
        OPEN (UNIT=33,ACCESS='SEQOUT',FILE='DATB.DAT')
c
c       file precpt.dat contains precip data for each day
c       file rechg.dat contains recharge values for each day
c
   1    read (31,101) n,lamda
 101    format (i3,f8.4)
        QINIT=63.0
        QOUT=34.8
        NN=N
        ZINIT=QINIT*60.0*24.0*.13368
        ZOUT= QOUT*60.0*24.0*.13368
        read (31,102) (date(1,i),date(2,i),q(i),i=1,nn)
 102    format (2a3,f5.1)
c
c
c       Change the flow from gpm to cu-ft per day
c
        NN=N
        do 69 k=1,nn
   69   Z(K)=Q(K)*60.0*24.0*.13368
c
c       Calculate the D-E with R=0 and set it equal to 'd'
c
        D(1)=3.*LAMDA*(Z(2)-ZINIT)+Z(2)+4.*Z(1)+ZINIT-LAMDA*
     1(Z(1)-ZINIT)-ZINIT
        D(N)=3.*LAMDA*(ZOUT-Z(N-1))+ZOUT+4.*Z(N)+Z(N-1)
     1-LAMDA*(ZOUT-Z(N))-ZOUT
        do 79 i=2,nn-1
  79    d(i)=3.0*LAMDA*(z(i+1)-z(i-1))+z(i+1)+4.0*z(i)+z(i-1)
c
c       Thomas algorithm for solving a tridigonal array
c
        bb(1)=4.0
        gg(1)=d(1)/4.0
        NN=N
        do 10 i=2,nn
        i1=i-1
        bb(i)=4.0-1.0/bb(i1)
  10    gg(i)=(d(i)-gg(i1))/bb(i)
c
c       Perform back substitution
c
        u(nn)=gg(nn)
        n1=nn-1
        do 15 j=1,n1
        i=nn-j
  15    u(i)=gg(i)-u(i+1)/bb(i)
        write (nunit,110)
 110    format (/5x,'RECHARGE ESTIMATES'///2x,'DATE',19x,
     &'RECHARGE',23x,'FLOW')
        NN=N
        do 22 i=1,nn
        write (32,760) I,u(i)
        write (33,761) z(i)
 760    format (' ',I3,2X,e12.6)
 761    format (' ',e12.6)
  22    WRITE (nunit,111) DATE(1,I),DATE(2,I),U(I),z(I),Q(I)
 111    format (1x,2a3,9x,e12.6,4x,9x,e12.6,4X,F4.1)
        close (unit=31)
        close (unit=32,device='dsk',access='seqout',
     &file='rechg.dat')
        close (unit=33,device='dsk',access='seqout',
     &file='DATB.dat')
   5    stop
        end
```

```
C       SOLUTION OF THE DAILY RECHARGE TERM USING A FINITE
C       DIFFERENCE APPROXIMATION
C
C       LAMDA    =  HYDRAULIC RESPONSE TIME
C       QINIT    =  ESTIMATED INITIAL SPRING FLOW  CU-FT / DAY
C       QOUT     =  ESTIMATED FINAL SPRING FLOW    CU-FT / DAY
C       Q        =  SPRING FLOW  CU-FT / DAY
C       R        =  CALCULATED RECHARGE  CU-FT / DAY
C
        DIMENSION Q(453),R(453)
        OPEN (UNIT=1,ACCESS='SEQIN',FILE='DAT8.DAT')
        OPEN (UNIT=20,ACCESS='SEQOUT',FILE='FDSPFL.DAT')
        QINIT=12127.45
        QOUT=6698.9722
        LAMDA=48.422202
        READ (1,100) (Q(I),I=1,453)
        R(1)=LAMDA/2.*(Q(2)-QINIT) + Q(1)
        R(453)=LAMDA/2.*(QOUT-Q(452)) + Q(453)
        DO 10 K=2,452
        R(K)=LAMDA/2.*(Q(K+1)-Q(K-1)) + Q(K)
   10   CONTINUE
        WRITE (20,200) (L,R(L),L=1,453)
        WRITE (5,200) (L,R(L),L=1,453)
  100   FORMAT (1X,E12.6)
  200   FORMAT (1X,I3,4X,E12.6)
        CLOSE (UNIT=1)
        CLOSE (UNIT=20)
        STOP
        END
```

Jan 04	.200158E+05	.201547E+05
Jan 05	.207435E+05	.203075E+05
Jan 06	.192961E+05	.186327E+05
Jan 07	.140966E+05	.150161E+05
Jan 08	.144714E+05	.145722E+05
Jan 09	.155868E+05	.160147E+05
Jan 10	.194669E+05	.184029E+05
Jan 11	.173326E+05	.176329E+05
Jan 12	.171280E+05	.176714E+05
Jan 13	.205433E+05	.196734E+05
Jan 14	.190422E+05	.193281E+05
Jan 15	.195857E+05	.189997E+05
Jan 16	.168670E+05	.172479E+05
Jan 17	.165904E+05	.163817E+05
Jan 18	.152080E+05	.150522E+05
Jan 19	.129137E+05	.136674E+05
Jan 20	.151417E+05	.155154E+05
Jan 21	.197865E+05	.188276E+05
Jan 22	.189967E+05	.184992E+05
Jan 23	.153885E+05	.167089E+05
Jan 24	.198490E+05	.190779E+05
Jan 25	.200400E+05	.192295E+05
Jan 26	.155471E+05	.165152E+05
Jan 27	.169729E+05	.165561E+05
Jan 28	.160321E+05	.166139E+05
Jan 29	.186776E+05	.180372E+05
Jan 30	.177526E+05	.172287E+05
Jan 31	.137148E+05	.144567E+05
feb 01	.141282E+05	.139935E+05
feb 02	.136968E+05	.135134E+05
feb 03	.121165E+05	.125702E+05
feb 04	.131224E+05	.138972E+05
feb 05	.188563E+05	.162469E+05
feb 06	.903139E+04	.107414E+05
feb 07	.904081E+04	.110121E+05
feb 08	.209507E+05	.184619E+05
feb 09	.181976E+05	.167270E+05
feb 10	.661506E+04	.931570E+04
feb 11	.108024E+05	.105104E+05
feb 12	.132738E+05	.133209E+05
feb 13	.158637E+05	.113959E+05
feb 14	-.846075E+04	-.112794E+05
feb 15	-.520262E+05	-.386324E+05
feb 16	-.180884E+05	-.175945E+05

feb 17	.182921E+05	.109532E+05
feb 18	.107444E+05	.962620E+04
feb 19	-.385352E+04	-.231000E+03
feb 20	.245727E+04	.404250E+04
feb 21	.182742E+05	.165538E+05
feb 22	.241784E+05	.231950E+05
feb 23	.249334E+05	.239662E+05
feb 24	.204033E+05	.190755E+05
feb 25	.818288E+04	.854690E+04
feb 26	-.239461E+04	-.480102E+03
feb 27	-.216948E+04	.635200E+03
feb 28	.143759E+05	.124547E+05
mar 01	.198665E+05	.159209E+05
mar 02	.160694E+04	.616000E+04
mar 03	.102575E+05	.921950E+04
mar 04	.128157E+05	.120709E+05
mar 05	.107875E+05	.106260E+05
mar 06	.781838E+04	.741000E+04
mar 07	.197516E+04	.306070E+04
mar 08	.224505E+04	.198270E+04
mar 09	.376439E+03	.313890E+04
mar 10	.147958E+05	.127435E+05
mar 11	.172679E+05	.179975E+05
mar 12	.244326E+05	.241202E+05
mar 13	.307131E+05	.263917E+05
mar 14	.116139E+05	.136482E+05
mar 15	.450984E+04	.660390E+04
mar 16	.971411E+04	.604450E+04
mar 17	-.743050E+04	-.286950E+04
mar 18	.171535E+04	.175170E+04
mar 19	.111309E+05	.829670E+04
mar 20	.312545E+04	.625620E+04
mar 21	.138533E+05	.118002E+05
mar 22	.123498E+05	.123019E+05
mar 23	.106056E+05	.109340E+05
mar 24	.107929E+05	.104515E+05
mar 25	.893392E+04	.906670E+04
mar 26	.769722E+04	.852890E+04
mar 27	.113793E+05	.989450E+04
mar 28	.610341E+04	.664000E+04
mar 29	.370016E+04	.464040E+04
mar 30	.667211E+04	.454420E+04
mar 31	-.350544E+04	-.115620E+04
apr 01	-.363112E+03	.128850E+04
apr 02	.125219E+05	.104924E+05
apr 03	.133435E+05	.133222E+05
apr 04	.142196E+05	.138600E+05

apr 05	.131328E+05	.125498E+05
apr 06	.861923E+04	.933620E+04
apr 07	.828185E+04	.881770E+04
apr 08	.111368E+05	.106633E+05
apr 09	.112015E+05	.125305E+05
apr 10	.194272E+05	.153819E+05
apr 11	.369997E+04	.627670E+04
apr 12	.276361E+04	.689030E+04
apr 13	.269050E+05	.204627E+05
apr 14	.130058E+05	.142450E+05
apr 15	.639012E+04	.998950E+04
apr 16	.215269E+05	.160737E+05
apr 17	.431411E+04	.513970E+04
apr 18	-.877650E+04	-.217410E+04
apr 19	.173324E+05	.138600E+05
apr 20	.232251E+05	.220015E+05
apr 21	.222963E+05	.217332E+05
apr 22	.186508E+05	.183067E+05
apr 23	.130998E+05	.146492E+05
apr 24	.171174E+05	.147647E+05
apr 25	.713695E+04	.787440E+04
apr 26	.119171E+04	.261800E+04
apr 27	.336527E+04	.290550E+04
apr 28	.239239E+04	.413870E+04
apr 29	.115947E+05	.109544E+05
apr 30	.172225E+05	.124740E+05
may 01	-.573613E+04	-.144380E+04
may 02	-.395940E+04	-.188650E+04
may 03	.100058E+05	.683274E+04
may 04	.474844E+04	.675695E+04
may 05	.113893E+05	.113199E+05
may 06	.173546E+05	.169783E+05
may 07	.194866E+05	.180745E+05
may 08	.130485E+05	.117629E+05
may 09	-.128752E+04	.242670E+04
may 10	.610526E+04	.588930E+04
may 11	.122786E+05	.105670E+05
may 12	.811766E+04	.960690E+04
may 13	.129184E+05	.119350E+05
may 14	.119545E+05	.115295E+05
may 15	.846307E+04	.119927E+05
may 16	.263239E+05	.222337E+05
may 17	.206237E+05	.203484E+05
may 18	.133337E+05	.138612E+05
may 19	.954497E+04	.939280E+04
may 20	.441127E+04	.456100E+04
may 21	.396365E+02	.365700E+03
may 22	-.325823E+04	-.193000E+02

may 23	.126879E+05	.114934E+05
may 24	.216678E+05	.208297E+05
may 25	.264224E+05	.234850E+05
may 26	.140808E+05	.167463E+05
may 27	.179212E+05	.135712E+05
may 28	-.419213E+04	-.161580E+04
may 29	-.121482E+05	-.589170E+04
may 30	.170699E+05	.120312E+05
may 31	.164230E+05	.131285E+05
jun 01	-.407573E+04	.595739E+03
jun 02	.265967E+04	.163645E+04
jun 03	.316210E+04	.487021E+04
jun 04	.134334E+05	.120514E+05
jun 05	.160489E+05	.155925E+05
jun 06	.158334E+05	.164395E+05
jun 07	.200189E+05	.163238E+05
jun 08	.190893E+04	.791050E+04
jun 09	.197900E+05	.171529E+05
jun 10	.224954E+05	.202137E+05
jun 11	.118414E+05	.147828E+05
jun 12	.190041E+05	.153037E+05
jun 13	.428499E+04	.435050E+04
jun 14	-.109215E+05	-.760500E+04
jun 15	-.711429E+04	-.887406E+04
jun 16	-.149625E+05	-.839280E+04
jun 17	.157904E+05	.134750E+05
jun 18	.336594E+05	.292032E+05
jun 19	.256549E+05	.253725E+05
jun 20	.167346E+05	.178255E+05
jun 21	.144412E+05	.150535E+05
jun 22	.162574E+05	.147828E+05
jun 23	.924034E+04	.875870E+04
jun 24	-.802515E+03	.848201E+03
jun 25	-.174907E+04	.499299E+03
jun 26	.105785E+05	.737270E+04
jun 27	.352518E+04	.408124E+04
jun 28	-.644988E+03	.203950E+04
jun 29	.109410E+05	.929771E+04
jun 30	.128932E+05	.987521E+04
jul 01	-.349347E+04	.236771E+04
jul 02	.148200E+05	.109532E+05
jul 03	.104485E+05	.750746E+04
jul 04	-.122879E+05	-.392704E+04
jul 05	.145688E+05	.143412E+05
jul 06	.409634E+05	.327825E+05
jul 07	.196081E+05	.203855E+05
jul 08	.280016E+04	.779740E+04
jul 09	.159814E+05	.115127E+05

Jul 10	.243528E+04	.554304E+04
Jul 11	.702802E+04	.808496E+04
Jul 12	.182499E+05	.156320E+05
Jul 13	.139736E+05	.170928E+05
Jul 14	.289199E+05	.219245E+05
Jul 15	.256822E+04	.648840E+04
Jul 16	-.120107E+04	.327370E+04
Jul 17	.221020E+05	.163613E+05
Jul 18	.112268E+05	.146095E+05
Jul 19	.208549E+05	.188457E+05
Jul 20	.190588E+05	.177304E+05
Jul 21	.940040E+04	.897050E+04
Jul 22	-.305065E+04	-.267700E+04
Jul 23	-.143251E+05	-.109916E+05
Jul 24	-.668239E+04	-.679505E+04
Jul 25	-.440449E+03	.789210E+03
Jul 26	.128897E+05	.947096E+04
Jul 27	.590002E+04	.679521E+04
Jul 28	.382727E+04	.288746E+04
Jul 29	-.407151E+04	.519710E+03
Jul 30	.148637E+05	.140717E+05
Jul 31	.301426E+05	.256795E+05
aus 01	.191297E+05	.184415E+05
aus 02	.450824E+04	.433121E+04
aus 03	-.121223E+05	-.627554E+04
aus 04	.573022E+04	.136671E+04
aus 05	-.291632E+04	-.596790E+03
aus 06	.166930E+04	.188646E+04
aus 07	.748110E+04	.465846E+04
aus 08	-.403548E+04	-.596050E+03
aus 09	.455421E+04	.612147E+04
aus 10	.227528E+05	.136287E+05
aus 11	-.135429E+05	-.798855E+04
aus 12	-.182767E+05	-.115498E+05
aus 13	.170958E+05	.101447E+05
aus 14	.110182E+05	.162662E+05
aus 15	.369827E+05	.322050E+05
aus 16	.360886E+05	.292790E+05
aus 17	-.528248E+04	.256021E+04
aus 18	-.362072E+03	.827710E+03
aus 19	.116485E+05	.823896E+04
aus 20	.311970E+04	.542846E+04
aus 21	.821513E+04	.764221E+04
aus 22	.997832E+04	.862396E+04
aus 23	.349989E+04	.579421E+04
aus 24	.106412E+05	.989446E+04
aus 25	.135485E+05	.123200E+05
aus 26	.920245E+04	.100485E+05

aus 27	.998631E+04	.100677E+05
aus 28	.113510E+05	.110302E+05
aus 29	.109322E+05	.101640E+05
aus 30	.591945E+04	.739196E+04
aus 31	.961078E+04	.872021E+04
sep 01	.807343E+04	.831596E+04
sep 02	.783195E+04	.870096E+04
sep 03	.129586E+05	.115500E+05
sep 04	.974134E+04	.111265E+05
sep 05	.149760E+05	.134942E+05
sep 06	.116408E+05	.113190E+05
sep 07	.632337E+04	.804646E+04
sep 08	.113343E+05	.108185E+05
sep 09	.134248E+05	.127435E+05
sep 10	.116224E+05	.118965E+05
sep 11	.115721E+05	.114730E+05
sep 12	.110680E+05	.115307E+05
sep 13	.134427E+05	.124932E+05
sep 14	.103487E+05	.102795E+05
sep 15	.673416E+04	.744971E+04
sep 16	.735399E+04	.743046E+04
sep 17	.829666E+04	.644871E+04
sep 18	-.199460E+04	-.770400E+02
sep 19	-.153742E+04	.519710E+03
sep 20	.111319E+05	.881646E+04
sep 21	.994713E+04	.102217E+05
sep 22	.105022E+05	.102602E+05
sep 23	.965906E+04	.102795E+05
sep 24	.126307E+05	.112420E+05
sep 25	.741119E+04	.852771E+04
sep 26	.873174E+04	.937471E+04
sep 27	.141078E+05	.131670E+05
sep 28	.140391E+05	.141680E+05
sep 29	.150696E+05	.133787E+05
sep 30	.607796E+04	.787321E+04
oct 01	.764997E+04	.731496E+04
oct 02	.722994E+04	.733421E+04
oct 03	.722256E+04	.862396E+04
oct 04	.157725E+05	.133210E+05
oct 05	.985185E+04	.106452E+05
oct 06	.862977E+04	.922071E+04
oct 07	.110304E+05	.111072E+05
oct 08	.139896E+05	.139177E+05
oct 09	.168768E+05	.159197E+05
oct 10	.143240E+05	.128012E+05
oct 11	.270869E+04	.450446E+04
oct 12	.134965E+04	.334946E+04
oct 13	.118844E+05	.979821E+04

oct 14	.998417E+04	.107607E+05
oct 15	.127971E+05	.126280E+05
oct 16	.148622E+05	.132059E+05
oct 17	.710499E+04	.816196E+04
oct 18	.548175E+04	.621771E+04
oct 19	.816144E+04	.848921E+04
oct 20	.127975E+05	.140332E+05
oct 21	.252839E+05	.202317E+05
oct 22	.807521E+04	.893196E+04
oct 23	-.458078E+04	-.105879E+04
oct 24	.346941E+04	.294521E+04
oct 25	.807174E+04	.791171E+04
oct 26	.118141E+05	.107415E+05
oct 27	.913617E+04	.935546E+04
oct 28	.777405E+04	.796946E+04
oct 29	.745354E+04	.791171E+04
oct 30	.986669E+04	.929771E+04
oct 31	.886598E+04	.883571E+04
nov 01	.764002E+04	.789246E+04
nov 02	.783633E+04	.785396E+04
nov 03	.808457E+04	.829671E+04
nov 04	.955692E+04	.873946E+04
nov 05	.611939E+04	.735346E+04
nov 06	.991181E+04	.100485E+05
nov 07	.147654E+05	.129360E+05
nov 08	.876036E+04	.974046E+04
nov 09	.860256E+04	.833521E+04
nov 10	.679195E+04	.692996E+04
nov 11	.562981E+04	.592896E+04
nov 12	.611124E+04	.679521E+04
nov 13	.105939E+05	.104527E+05
nov 14	.144373E+05	.142450E+05
nov 15	.174141E+05	.162085E+05
nov 16	.135805E+05	.131477E+05
nov 17	.715265E+04	.850846E+04
nov 18	.881093E+04	.756521E+04
nov 19	.285890E+04	.381146E+04
nov 20	.221426E+04	.271421E+04
nov 21	.430513E+04	.400396E+04
nov 22	.430168E+04	.435046E+04
nov 23	.438572E+04	.565946E+04
nov 24	.119609E+05	.106837E+05
nov 25	.121630E+05	.112805E+05
nov 26	.701854E+04	.846996E+04
nov 27	.106160E+05	.941321E+04
nov 28	.700180E+04	.802721E+04
nov 29	.945280E+04	.937471E+04
nov 30	.115559E+05	.112805E+05

dec 01	.121090E+05	.117810E+05
dec 02	.108787E+05	.109340E+05
dec 03	.100006E+05	.100100E+05
dec 04	.926601E+04	.866246E+04
dec 05	.478950E+04	.583271E+04
dec 06	.638239E+04	.714171E+04
dec 07	.125107E+05	.991371E+04
dec 08	.314417E+04	.440821E+04
dec 09	.848660E+03	.279121E+04
dec 10	.101034E+05	.831596E+04
dec 11	.862841E+04	.877796E+04
dec 12	.805076E+04	.831596E+04
dec 13	.902074E+04	.968271E+04
dec 14	.140883E+05	.106645E+05
dec 15	-.132824E+04	.837371E+04
dec 16	.413848E+05	.277392E+05
dec 17	.408966E+04	.408096E+04
dec 18	-.354366E+05	-.205395E+05
dec 19	.137875E+05	.471646E+04
dec 20	.854281E+04	.102600E+05
dec 21	.137770E+05	.121850E+05
dec 22	.965554E+04	.104142E+05
dec 23	.101067E+05	.995221E+04
dec 24	.976198E+04	.954796E+04
dec 25	.810494E+04	.860471E+04
dec 26	.948506E+04	.908596E+04
dec 27	.847575E+04	.862396E+04
dec 28	.835571E+04	.816196E+04
dec 29	.702954E+04	.721871E+04
dec 30	.674604E+04	.671821E+04
dec 31	.619812E+04	.621771E+04
Jan 01	.562667E+04	.616020E+04
Jan 02	.815239E+04	.796947E+04
Jan 03	.961395E+04	.845071E+04
Jan 04	.405761E+04	.612171E+04
Jan 05	.107048E+05	.974023E+04
Jan 06	.118508E+05	.112610E+05
Jan 07	.945141E+04	.103180E+05
Jan 08	.124643E+05	.113382E+05
Jan 09	.878983E+04	.997146E+04
Jan 10	.122975E+05	.109340E+05
Jan 11	.776507E+04	.821971E+04
Jan 12	.580137E+04	.721871E+04
Jan 13	.123649E+05	.109340E+05
Jan 14	.105226E+05	.916296E+04
Jan 15	.412177E+03	.217545E+04
Jan 16	.384816E+03	.103971E+04
Jan 17	.401093E+04	.371522E+04

Jan 18	.561904E+04	.639097E+04
Jan 19	.118767E+05	.105682E+05
Jan 20	.104630E+05	.972122E+04
Jan 21	.457558E+04	.600597E+04
Jan 22	.709012E+04	.777697E+04
Jan 23	.138329E+05	.119927E+05
Jan 24	.976709E+04	.977897E+04
Jan 25	.571084E+04	.743047E+04
Jan 26	.119621E+05	.106642E+05
Jan 27	.106457E+05	.102987E+05
Jan 28	.722957E+04	.843147E+04
Jan 29	.110633E+05	.983647E+04
Jan 30	.762968E+04	.802745E+04
Jan 31	.646059E+04	.704571E+04
feb 01	.878539E+04	.750747E+04
feb 02	.335538E+04	.469697E+04
feb 03	.570291E+04	.642947E+04
feb 04	.124663E+05	.106260E+05
feb 05	.832872E+04	.883572E+04
feb 06	.716122E+04	.741122E+04
feb 07	.748348E+04	.741122E+04
feb 08	.728493E+04	.783472E+04
feb 09	.104185E+05	.923997E+04
feb 10	.652972E+04	.694922E+04
feb 11	.498857E+04	.502422E+04
feb 12	.350994E+04	.404247E+04
feb 13	.494938E+04	.531297E+04
feb 14	.853962E+04	.808497E+04
feb 15	.940195E+04	.900897E+04
feb 16	.799360E+04	.766147E+04
feb 17	.447182E+04	.529372E+04
feb 18	.573518E+04	.523597E+04
feb 19	.385703E+04	.471622E+04
feb 20	.694418E+04	.648722E+04
feb 21	.731269E+04	.650647E+04
feb 22	.267451E+04	.411947E+04
feb 23	.651110E+04	.542847E+04
feb 24	.378779E+04	.448522E+04
feb 25	.498222E+04	.529372E+04
feb 26	.805853E+04	.808497E+04
feb 27	.112986E+05	.103950E+05
feb 28	.937863E+04	.912447E+04
mar 01	.583355E+04	.675672E+04
mar 02	.785573E+04	.677597E+04
mar 03	.327358E+04	.487022E+04
mar 04	.812504E+04	.758447E+04
mar 05	.984857E+04	.902822E+04
mar 06	.666537E+04	.764222E+04

mar 07	.934327E+04	.810422E+04
mar 08	.463050E+04	.581347E+04
mar 09	.680259E+04	.617922E+04
mar 10	.529611E+04	.621772E+04
mar 11	.911141E+04	.889347E+04
mar 12	.119424E+05	.104335E+05
mar 13	.567337E+04	.577497E+04
mar 14	-.835993E+02	.654470E+03
mar 15	-.198947E+04	-.519780E+03
mar 16	.468173E+04	.356122E+04
mar 17	.443490E+04	.579422E+04
mar 18	.123671E+05	.108955E+05
mar 19	.117799E+05	.110302E+05
mar 20	.677405E+04	.735347E+04
mar 21	.520623E+04	.502422E+04
mar 22	.236675E+04	.356122E+04
mar 23	.649912E+04	.533222E+04
mar 24	.360960E+04	.394622E+04
mar 25	.243444E+04	.288747E+04
mar 26	.385438E+04	.331097E+04
mar 27	.174193E+04	.227147E+04
mar 28	.260154E+04	.265647E+04
mar 29	.353214E+04	.394622E+04
mar 30	.679800E+04	.623697E+04
mar 31	.667256E+04	.669897E+04
apr 01	.670557E+04	.669902E+04

STOP